P2

NASA CR-132311

FABRICATION AND PROPERTIES OF GALLIUM PHOSPHIDE VARIABLE COLOUR DISPLAYS

by

D. Effer, R.A. MacDonald, G.M. MacGregor,
W.A. Webb, and D.I. Kennedy

FINAL REPORT

July 1973

(NASA-CR-132311) FABRICATION AND PROPERTIES OF GALLIUM PHOSPHIDE VARIABLE COLOUR DISPLAYS Final Report, May 1972 - Jul. 1973 (Bowmar Canada, Ltd.) ~~52~~ 56 p HC CSCL 20L G3/26

N74-12434

Unclas 22741

Prepared Under Contract No. NASI-11523

by

Research & Development Division
Bowmar Canada Limited
Ottawa, Canada

for

Langley Research Center
Hampton, Virginia
National Aeronautics and Space Administration

Dr. Roger Crouch
Technical Representative
NASI-11523
Langley Research Center
Mail Stop 473
Hampton, Virginia 23365

Requests for copies of this report should be referred to:

NASA Scientific and Technical Information Facility
P.O. Box 33, College Park, Maryland 20740

1. Report No.	2. Government Accession No.	3. Recipient's Catalog No.
NASA CR-132311		

4. Title and Subtitle	5. Report Date
Fabrication and Properties of Gallium Phosphide Variable Colour Displays	July 1973
	6. Performing Organization Code
7. Author(s) D. Effer, R.A. MacDonald, G.M. MacGregor, W.A. Webb, and D.I. Kennedy	8. Performing Organization Report No.
9. Performing Organization Name and Address Research & Development Division Bowmar Canada Limited 1257 Algoma Road Ottawa, Canada	10. Work Unit No.
	11. Contract or Grant No. NASI-11523
12. Sponsoring Agency Name and Address National Aeronautics and Space Administration Washington, D.C. 20546	13. Type of Report and Period Covered Final Report May 1972 - July 1973
	14. Sponsoring Agency Code

15. Supplementary Notes

16. Abstract

The unique properties of single-junction gallium phosphide devices incorporating both red and green radiative recombination centers were investigated in application to the fabrication of monolithic 5 x 7 displays capable of displaying symbolic and alphanumeric information in a multicolor format. A number of potentially suitable material preparation techniques were evaluated in terms of both material properties and device performance. Optimum results were obtained for a double liquid-phase-epitaxial process in which an open-tube "dipping" technique was used for n-layer growth and a sealed "tipping" procedure for subsequent p-layer growth. It was demonstrated that to prepare devices exhibiting a satisfactory range of dominant wavelengths which can be perceived as distinct emission colors extending from the red through green region of the visible spectrum involves a compromise between the material properties necessary for efficient red emission and those considered optimum for efficient green emission. Compatible red/green emission characteristics were obtained for a $n:p^+$ device structure in which the n-side of the junction was doped with tellurium and nitrogen and the p-side with zinc and oxygen. Quantum efficiency values for the two emission bands in a typical multicolor display were 1.0 to 1.5% for the red component (at a current density of $3A/cm^2$) and 0.01 to 0.02% for the green component (at a current density of $250A/cm^2$). Suitable procedures were developed for the fabrication of 5 x 7 matrices which accommodated the requirement for X-Y addressing of the array while at the same time minimizing crosstalk between segments. By operating the 5 x 7 displays under drive conditions which extended from low-current, high duty-cycle, to high-current, low duty-cycle, an acceptable range of emission colors were generated which ranged from red, through orange and yellow, to green; associated surface luminance values exceeded 250 ft-L at average currents of 5mA/segment. A demonstration Information Display System incorporating three 5 x 7 multicolor displays was constructed which was capable of displaying the 64-character ASCII code in a variety of color combinations. The system also incorporated separate pure-red and pure-green emitting 5 x 7 gallium phosphide displays to allow comparative evaluation of the color performance of the multicolor displays.

17. Key Words (Selected by Author(s))	18. Distribution Statement
GaP, LPE Variable Color LED's 5 x 7 Alphanumeric Arrays Multicolor Information Display System	**Distribution of this report is provided in the interest of information exchange and should not be construed as endorsement by NASA of the material presented. Responsibility for the contents resides with the organization that prepared it.**

19. Security Classif. (of this report)	20. Security Classif. (of this page)	21. No. of Pages	22. Price*
Unclassified	Unclassified	51	

*For sale by the Clearinghouse for Federal Scientific and Technical Information, Springfield, Virginia 22151.

PRECEDING PAGE BLANK NOT FILMED

FABRICATION AND PROPERTIES OF GALLIUM PHOSPHIDE VARIABLE COLOUR DISPLAYS

by

D. Effer, R.A. MacDonald, G.M. MacGregor,
W.A. Webb, and D.I. Kennedy

SUMMARY

The unique properties of single-junction gallium phosphide devices incorporating both red and green radiative recombination centers were investigated in application to the fabrication of monolithic 5 x 7 displays capable of displaying symbolic and alphanumeric information in a multicolor format.

A number of potentially suitable material preparation techniques were evaluated in terms of both material properties and device performance. Optimum results were obtained for a double liquid-phase-epitaxial process in which an open-tube "dipping" technique was used for n-layer growth and a sealed "tipping" procedure for subsequent p-layer growth.

It was demonstrated that to prepare devices exhibiting a satisfactory range of dominant wavelengths which can be perceived as distinct emission colors extending from the red through green region of the visible spectrum involves a compromise between the material properties necessary for efficient red emission and those considered optimum for efficient green emission. Compatible red/green emission characteristics were obtained for a $n:p^+$ device structure in which the n-side of the junction was doped with tellurium and nitrogen and the p-side with zinc and oxygen. Quantum efficiency values for the two emission bands in a typical multicolor display were 1.0 to 1.5% for the red component (at a current density of $3A/cm^2$) and 0.01 to 0.02% for the green component (at a current density of $250A/cm^2$).

Suitable procedures were developed for the fabrication of 5 x 7 matrices which accommodated the requirement for X-Y addressing of the array while at the same time minimizing crosstalk between segments. By operating the 5 x 7 displays under drive conditions which extended from low-current, high duty-cycle, to high-current, low duty-cycle, an acceptable range of emission colors were generated which ranged from red, through orange and yellow, to green; associated surface luminance values exceeded 250 ft-L at average currents of 5mA/segment.

A demonstration Information Display System incorporating three 5 x 7 multicolor displays was constructed which was capable of displaying the 64 character ASCII code in a variety of color combinations. The system also incorporated separate pure-red and pure-green emitting 5 x 7 gallium phosphide displays to allow comparative evaluation of the color performance of the multicolor displays.

TABLE OF CONTENTS

TABLE OF CONTENTS

I INTRODUCTION

The technology of semiconductor light-emitting-devices has become fully established in recent years. Discrete devices and simple numeric and alphanumeric displays are widely utilized in a variety of display applications, both commercial and military. The technology is also being used for the fabrication of more complex displays, particularly in applications where high reliability, long life, and low-voltage drive requirements are a prerequisite. The most commonly used display materials are red-emitting GaAsP and GaP. The former is more widely used for the fabrication of complex arrays due to its compatibility with planar technology and its high self-absorption coefficient which permits the fabrication of monolithic, high-resolution displays without resort to complex optical isolation procedures.

The commercial introduction of yellow- and green-emitting III-V compound materials has considerably expanded the potential number of applications which can be envisaged for LED displays. One prospective application which can now be realized is the fabrication of multicolor displays. The ideal primary color combinations which are readily amenable to material processing and display fabrication techniques are not available in LED materials; therefore, independent of economic considerations, LED displays do not offer an effective alternative to existing multicolor display systems. However, it is now feasible to construct LED displays emitting in the red through green region of the visible spectrum. In relation to the color latitude required for data or scientific information systems, it is advantageous to eliminate any blue component from the display. By mixing the red and green components in the proper ratios, orange and yellow can be produced. Four distinct colors are adequate for a comprehensive multicolor information display system.

Several fabrication techniques can be selected for displays emitting in the red through green region. These include simple two-terminal single-junction structures, dual-junction three-terminal networks, and hybrid assemblies of isolated devices emitting in different regions of the spectrum. The combined processing technology, assembly procedures, and associated drive circuitry requirements become progressively more complex for each type of display.

For displays based on GaP, it is possible to capitalize on the unique behaviour of the red-emission band in GaP - namely its tendency to saturate with increasing current density - to effect a change in visual emission color as a function of applied current density in devices incorporating both red and green radiative recombination centers.

This report discusses the characteristics, both optical and electrical, of two-terminal single-junction multicolor devices, followed by a description of relevant material preparation procedures and display fabrication techniques developed to accommodate the program specifications. It concludes with a presentation of the performance characteristics of a multicolor display system in which the 5 x 7 arrays are integrated with a suitable electronics package. It should be pointed out at this juncture that although the electronic drive and addressing circuitry for single-junction multicolor devices must be designed and operated in a manner distinctly variant from conventional LED displays, the inherent complexity is not significantly greater than techniques which must be adopted for the multiplex addressing of other single-color LED displays.

II PERFORMANCE CHARACTERISTICS OF SINGLE-JUNCTION GaP MULTICOLOR DISPLAYS

In this section the unique properties of GaP multicolor displays are reviewed in terms of the salient electro-optical characteristics of the material. Details of the specific material processing and device fabrication procedures developed under the present program will be discussed in subsequent sections.

Figure 1 shows the two major emission bands commonly observed in GaP devices. The red-emission band centered at 6950Å results from the radiative recombination of electron-hole pairs at nearest neighbour Zn-O isoelectronic centers occupying Ga and P sites, respectively, (Ref. 1). The radiative recombination takes place primarily in the p-type material (Ref. 2). Depending on the injection efficiency of the p-n junction, the minority carrier diffusion length, and the concentration of Zn-O complexes and non-radiative centers in the vicinity of the junction, the radiative recombination process saturates at a certain current density. In terms of external quantum efficiency (defined as the number of photons generated per electron flowing across the junction) this is manifested by a low-current maxima and subsequent reduction in the value of this parameter for the red emission band. Thus the luminous intensity of the red emission band increases with voltage more slowly than the diode current, resulting in a sublinear increase of red intensity with current.

The green emission band in GaP is located in the region of 5650Å for material doped with nitrogen in the $10^{18}cm^{-3}$ -$10^{19}cm^{-3}$ range. The predominant recombination process in nitrogen-doped material involves exciton recombination at the trap created by the substitution of isoelectronic nitrogen for phosphorus in the GaP lattice (Ref. 3). The dependence of luminous emission intensity on current density for the green emission band in GaP devices is superlinear in current over the current range where series resistance effects are not a significant limiting factor. The external quantum efficiency therefore exhibits a monotonic increase with increasing current over the operating range selected for this type of device. Characteristics typical of a discrete multicolor device are illustrated in Figures 2 and 3. In Figure 2, the dependence of external quantum efficiency on current density has been determined for both red and green emission bands. Two sets of drive conditions are employed, one to enhance the red component, and the other the green component. It will be noted that under conditions referred to as the 'red mode', 1Kcps 15% duty cycle, the external quantum efficiency of the red component maximizes at a current level of approximately 3mA ($1.2A/cm^2$) and subsequently falls. In contrast, the external quantum efficiency of the green component progressively increases throughout the same current range. To induce a predominantly green coloration and permit operation of the device at elevated current levels, the duty cycle is altered from 15% to 0.8%. Under these conditions, the device can be operated at peak current levels of 600mA without noticeable resistive-heating effects. Under the high current conditions, the external quantum efficiency of the red band is reduced by up to an order of magnitude in comparison with the low current value, whereas the green component progressively increases, typically with a one-quarter to one-third power dependence on current density; the high current value is normally three times that obtained at low current levels. The ratios of red to green external quantum efficiencies are normally 300:1 at the red emission efficiency maximum, reducing to 10:1 at high current levels. To obtain adequate surface luminance

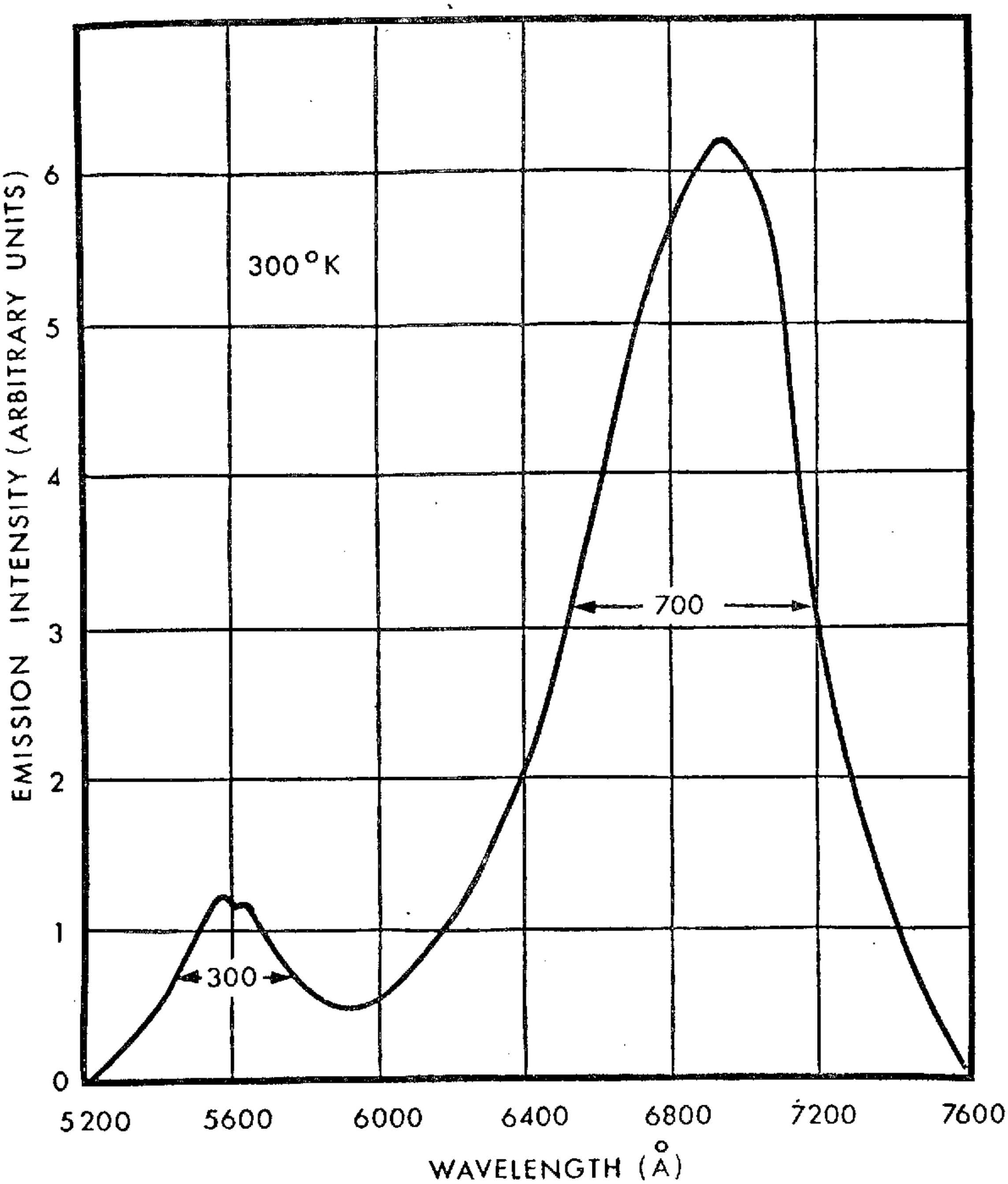

Figure 1 Typical Emission Spectrum of a GaP Device Prepared Using Liquid-Phase-Epitaxial Techniques

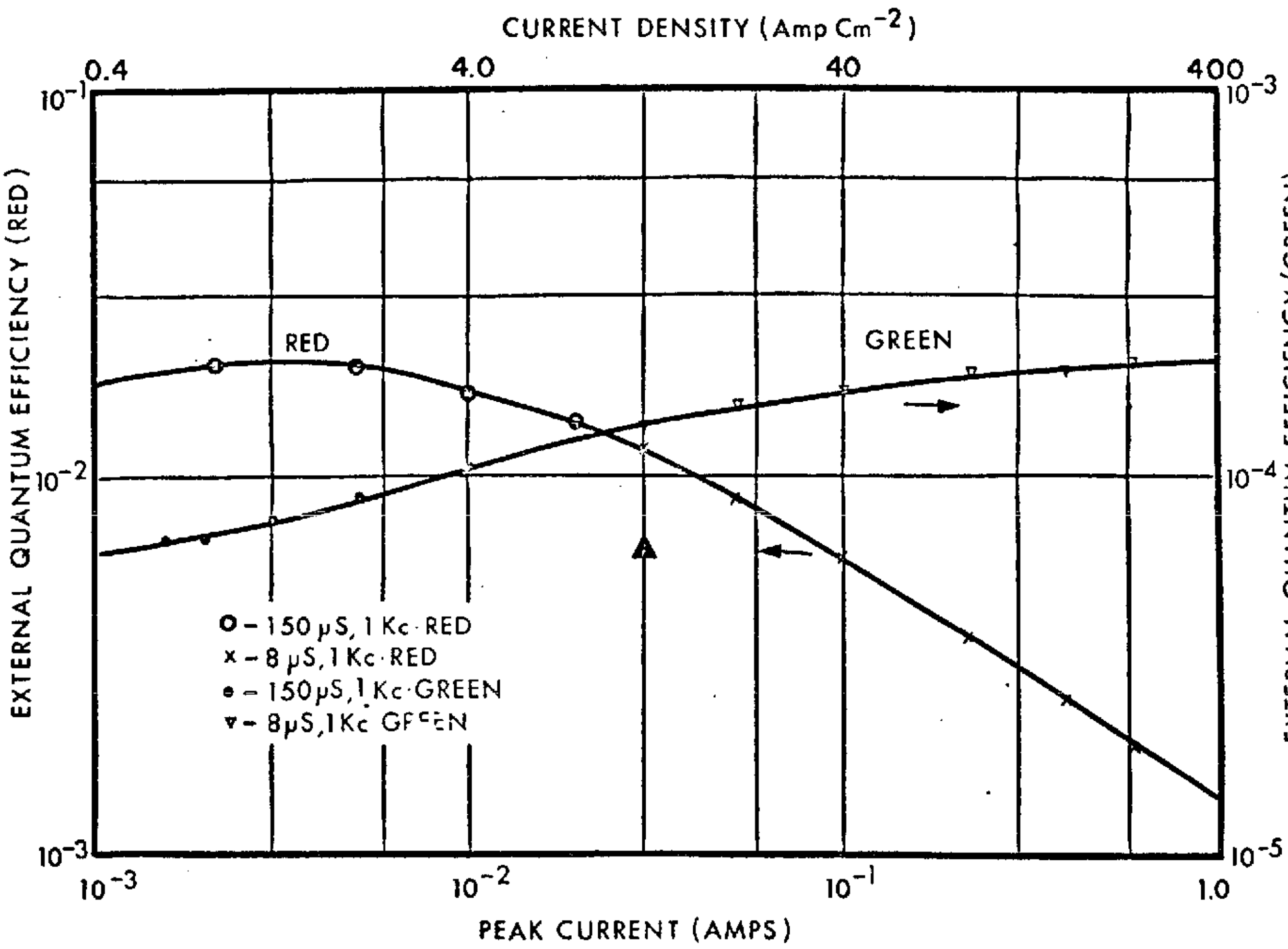

Figure 2 External Quantum Efficiency Versus Operating Current For A Red:Green GaP Device (Device Area 2.5 x 10^{-3}cm^2)

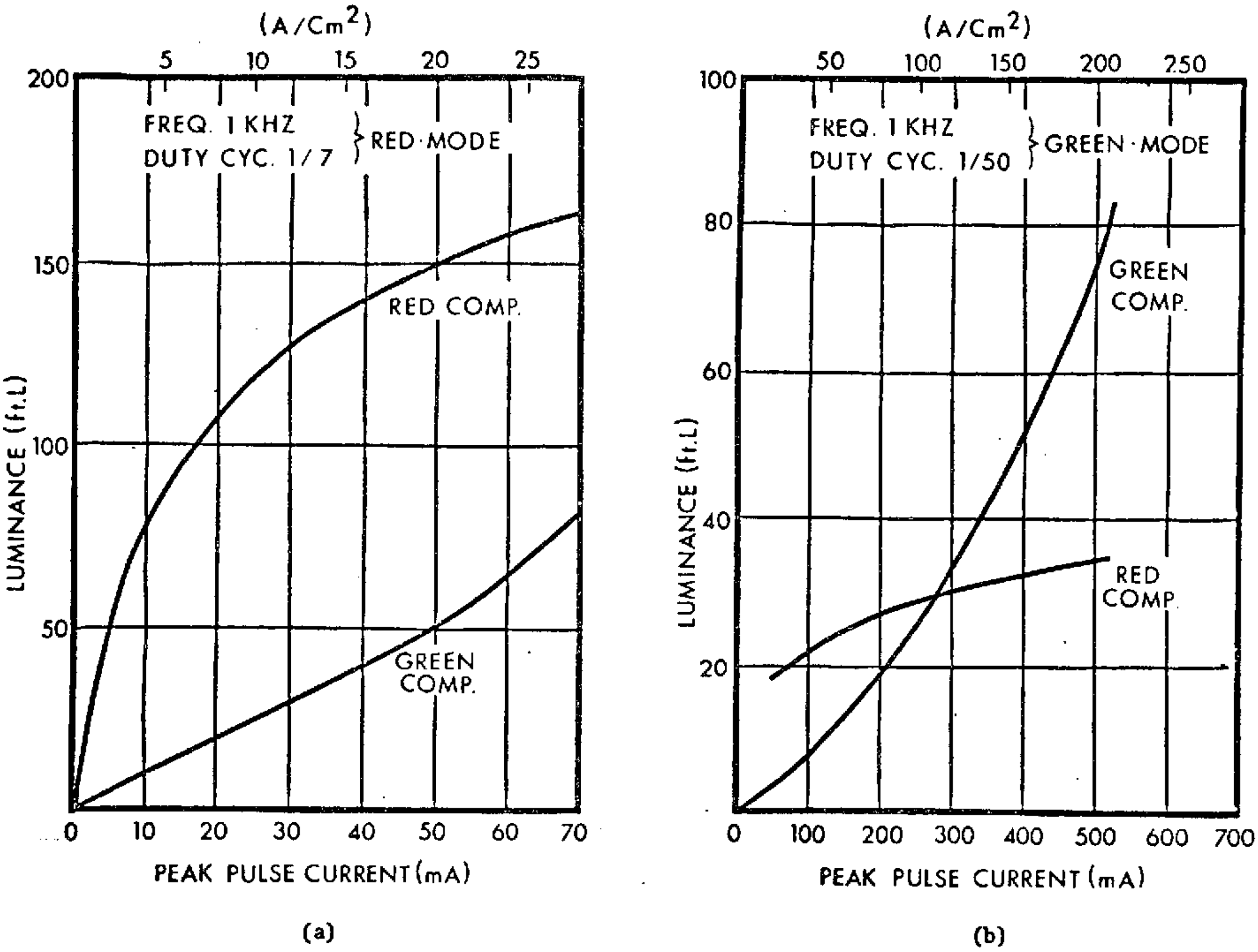

Figure 3 Dependence Of Surface Brightness On Peak Pulse Current For A BCL Red/Green GaP Device. (The Individual Red and Green Components Of The Emission Spectrum Were Measured Separately)

(a) Drive Conditions Selected For Red-Mode Operation

(b) Drive Conditions Selected For Green-Mode Operation (brightness) levels, devices are not operated at current levels corresponding to the maxima of the red external quantum efficiency, but at current densities in the range $5A/cm^2$ to $10A/cm^2$. At this level, the red to green efficiency ratio is approximately 60% of the maximum value. The performance in terms of the dependence of surface luminance (ft-L) on current is depicted in Figures 3(a) and 3(b).

From Figure 1, it is observed that the half-width of the red emission band is approximately 700Å. Correction for the sensitivity of the human eye results in a modified spectrum peaking at 6500Å. The green emission band is more monochromatic, 300Å in half-width, and correction for eye sensitivity does not significantly modify the peak position. Depending on the relative magnitude of the two emission bands in GaP, the subjectively determined emission color, or visual hue, can be made to vary from red to green. Since the eye is approximately thirty times more sensitive to the green emission band than the red, equivalent values of luminous intensity are achieved for significantly lower values of green external quantum efficiency.

The actual device performance is based on three critical parameters:

(1) Red Efficiency
(2) Green Efficiency
(3) Red Saturation Characteristics (i.e. the current density at which the dependence of red emission intensity on current density becomes sublinear in current).

By controlled selection of these parameters, a device can be fabricated which appear visually red at low current density, orange-yellow at intermediate current density and green at high current density. As mentioned above, due to the eye sensitivity to green emission, it is necessary for the external quantum efficiency of the green component to be significantly lower than the red component.

Since the brightness attained is a function of the average current and the visual color is dependent on the peak current, the two color requirement necessitates operation in a pulse mode with two distinct duty cycles. This is not considered a disadvantage since the majority of visual LED displays are operated using multiplexed X-Y addressing. The actual brightness levels attained under the selected pulsed operating conditions are dictated by the emission efficiency values for the two components. One positive advantage of the pulsed drive operation is the capability to uniformly modulate brightness by reducing the pulse width from the maximum value. This is a much more satisfactory method of dimming an array than reducing the peak current. The latter might result in uniformity variation and, most important, color distortion.

The subjective evaluation of hue and saturation can best be quantitatively assessed by calculating their corresponding respective colormetric parameters-dominant wavelength (color clarity) and purity.

Color purity can be derived from the calculated tristimulus values for the emitted spectrum. This calculation is based on the emitted radiated spectrum and the CIE color matching function. The sensation of brightness is proportional to the Y tristimulus coordinate which varies as the radiated power of a fixed spectrum. This can be converted to a corresponding luminous efficiency. Dominant wavelength and purity are determined from the chromaticity coordinates determined from the tristimulus values or corresponding tristimulus luminous efficiencies.

The chromaticity coordinates for the red and green emission bands in GaP have been determined previously (Ref. 4). The dominant emission wavelength for 100% red purity is 6370Å with a corresponding luminous efficiency of 20 lumens/watt; and for the green, 5700Å, with an efficiency of 620 lumens/watt. Using these values, the chromaticity coordinates and corresponding luminous efficiency values for any combination of red and green intensity can be calculated.

The red:green luminous efficiency, K_{yRG}, as a function of green:red radiated power ratio P_G/P_R is shown in Figure 4(a). From this data, it is apparent that for a small change in P_G/P_R ratio, the luminous efficiency increases markedly over the value for red alone due to the much higher green luminous efficiency. Figure 4(b) shows the dependence of dominant wavelength on R/G ratio. This figure depicts the eye response or subjective color in terms of the relative intensity of the two emission bands. Thus, under ideal conditions, the visual hue can vary from pure red (6370Å) to pure green (5700Å). For a practical multicolor device operated under drive conditions selected to maximize the red component, it is not possible to exclude a finite green component, and conversely when operated under 'green' drive conditions, a residual red component. Thus the two extreme 'pure' components indicated in the figure cannot be achieved in a single-junction device. Nevertheless, the degree of color selectivity attainable in this device structure is sufficiently well-defined to permit the controlled selection of a range of visual hues ranging from an acceptable deep red coloration to a distinctive yellow-green.

The red:green performance of an experimental device can be determined from the above data and a measurement of the current density dependence of P_R and P_G. For this purpose, the luminance data of Figure 3 can be used as a basis for computation of the $P_G:P_R$ ratio. The result, shown in Figure 5, also includes the perceived hue corresponding to the dominant wavelength values and allows the evaluation of this parameter as a function of peak current density. Two sets of operating conditions were used to generate the figure, one selected to enhance the red component and the other the green component. The active junction area presented is typical of that used in hybrid multicolor display applications ($2.5 \times 10^{-3} cm^2$). In normal operation, the visual color under drive conditions selected to develop a predominantly red coloration corresponded to a wavelength of approximately 6250Å, and under conditions selected to generate a predominantly green coloration, 5750Å.

It should be pointed out that the drive conditions chosen to induce the red and green emission characteristics in GaP devices can be significantly modified from those used here to demonstrate typical device performance. Indeed the optimum operating mode for the red emission band is obviously d.c. and for the green emission band the shortest pulse duration and highest peak current

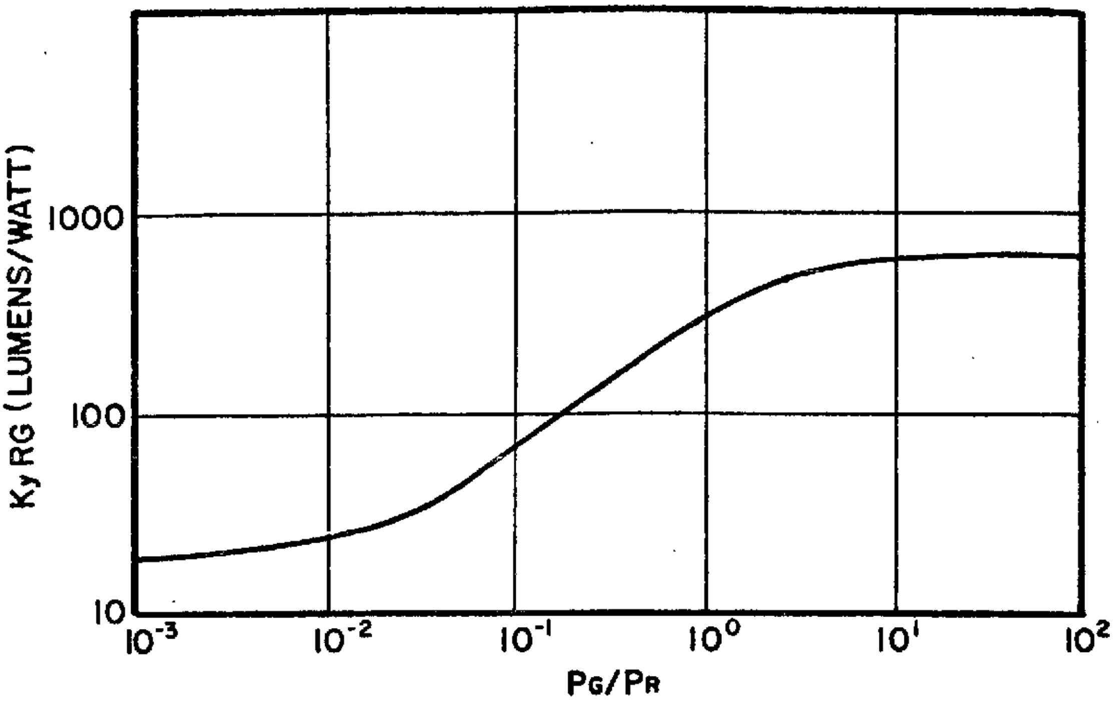

(a)

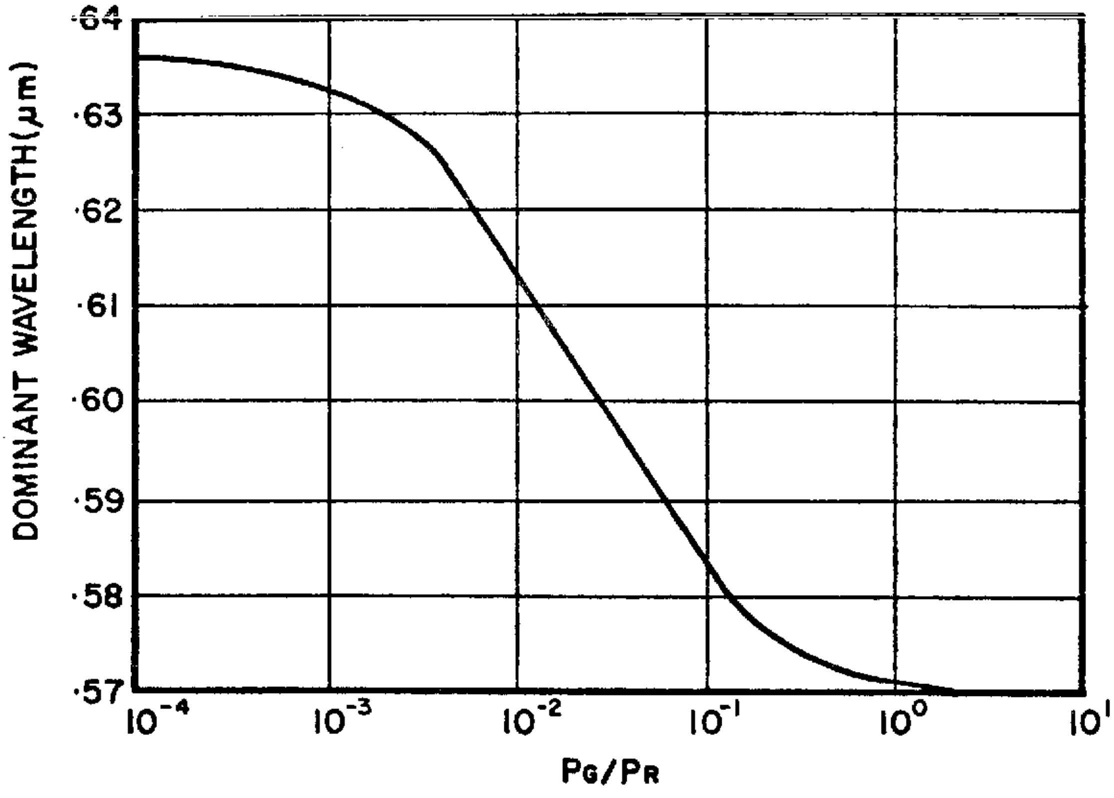

(b)

Figure 4 (a) Dependence of Red:Green Luminous Efficiency As A Function of Green:Red Radiated Power Ratio $P_G:P_R$

(b) Dominant Wavelength As A Function of Green:Red Radiated Power Ratio $P_G:P_R$

- after Logan et al. (Ref. 4)

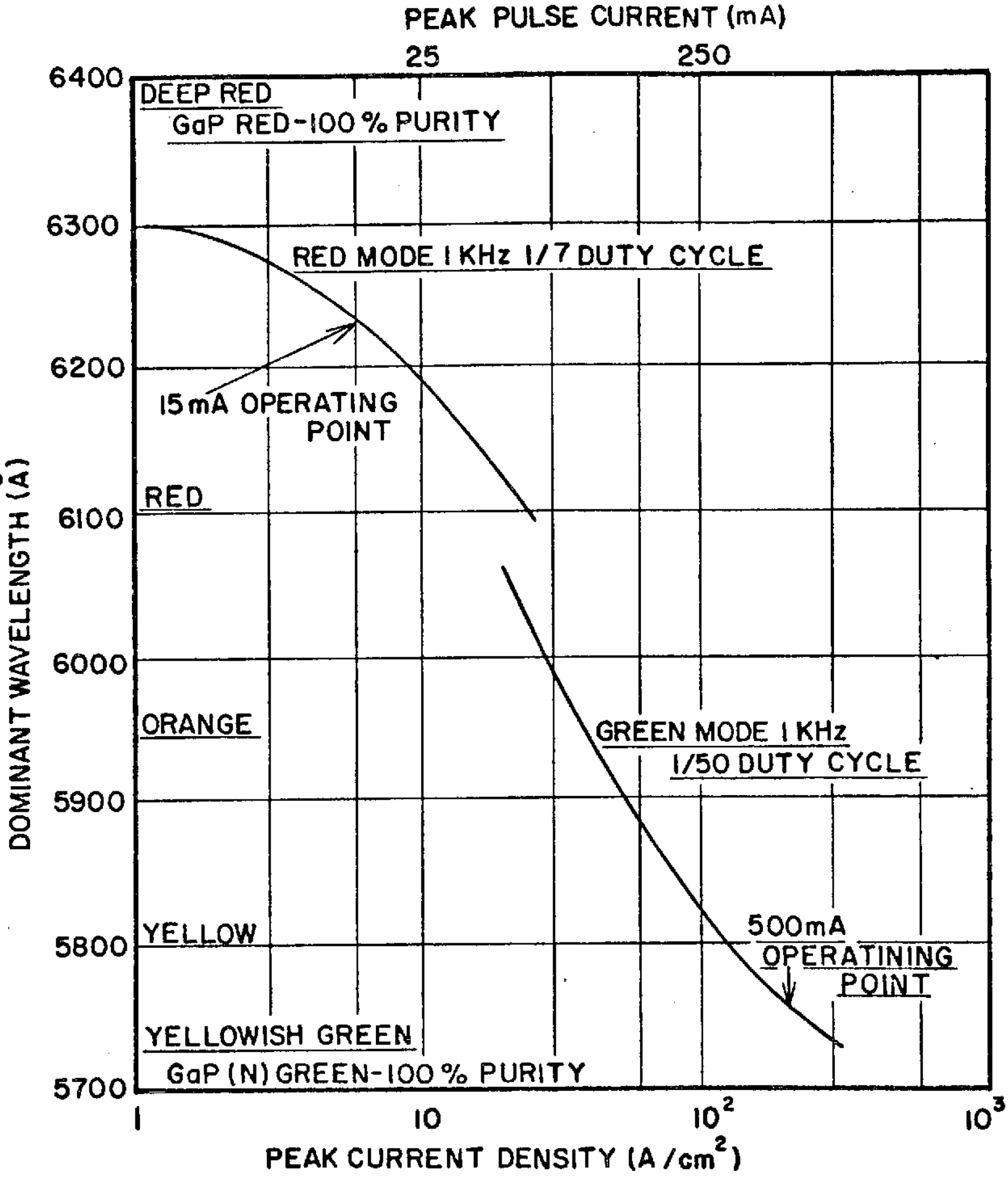

Figure 5 Dependence Of Dominant Wavelength On Peak Current Density For A BCL Red/Green GaP Device

consistent with considerations of adequate device performance - as evaluated in terms of spreading resistance, resistive heating, instantaneous junction temperature, and other associated defect and impurity mechanisms which contribute to device degradation (Ref. 5). Obviously, in practical applications, it is important to select operating conditions which do not induce accentuated degradation of one emission band in comparison with the other. Considerable flexibility exists in the choice of device operating frequency; this parameter is selected to be consistent with the multiplexing conditions and element density of any particular array of multicolor devices.

III MATERIAL PREPARATION

1. p-n Junction Formation by Diffusion Processes

The possibility of producing practical red/green emissions from diffused junctions in n-type GaP grown on L.E.C. substrates was examined in conjunction with exploratory programs of double-L.P.E. growth. General direction of work programs was based on the initial assessment of all the possible methods and their potential in achieving the contract aims. In this respect, diffusion processes were found to be inferior to the double-L.P.E. procedures. However it is not suggested that these techniques will not prove useful as material properties improve and a more thorough understanding of red/green emitting junctions is obtained. Certainly planar diffusion procedures provide a versatile design capability which could be exploited effectively in application to monolithic multicolor display processing.

A. Out-Diffusion - Intermediate efficiency (0.5%) red-emitting GaP diodes have been prepared in these laboratories by the process in which a Zn,O, and Te doped L.P.E. layer (over-compensated with Zn) is grown on a p-type GaP substrate, either solution or L.E.C. grown. Annealing of the grown layer in the gallium melt either during growth, for layers grown at relatively slow rates (0.25°C/min.), or after growth for layers grown at rates in excess of 1°C/min., allows Zn to diffuse from the surface layer of the crystal into the gallium thus forming a shallow out-diffused junction (Ref. 6).

For a red/green emitting junction, both nitrogen (from GaN) and oxygen (from Ga_2O_3) were introduced into melts containing Te, over-compensated with Zn, and out-diffused junctions prepared by either a final 1 hour heat treatment at 800°C, giving a 3μ junction, or 2 hours at 900°C, giving an 18μ junction. The junction depths were the same for in-situ diffusions in the Ga melt or after the material had been cleaned and transferred to an evacuated ampoule. In compensated out-diffused junctions prepared in this way carrier injection into the p-region is predominant. Red/green emissions were obtained, but of low intensity corresponding to a red efficiency of less than 0.3% and a green efficiency level in the low 10^{-3}% range. Annealing for 16 hrs. at 500°C had the effect of increasing the red emission effectively without affecting the green component.

Apart from these performance restrictions, out-diffusion techniques are not readily amenable to selective junction formation procedures.

B. In-Diffusion - The planar process for the fabrication of L.E.D. arrays has obvious advantages over processes which depend on mechanical and/or chemical separation of individual diode elements on a monolithic block.

For these diffusion experiments, a series of variously doped Te, N, and O doped n-layers were prepared on L.E.C. substrates by the tipping process.

Various diffusion schedules were utilized using both Zn and Zn_3P_2 diffusion sources. Diffusion schedules investigated extended from 15 min. at 875°C to 120 min. at 950°C; in certain cases, a 600Å modulating oxide was deposited on one surface of the wafers prior to diffusion. Junction depths ranged from 6 to 12 microns. Sample diodes were prepared for the various diffusion schedules and emission intensities were examined in both d.c. and pulsed modes. Details of the material and device evaluations are not presented here since the results did not accommodate the required specification.

2. Efficient Red/Green Junction Formation - General Considerations

The requirements for the preparation of efficient red - or green-emitting L.P.E. junctions in GaP have been extensively reported. The optimization of junction properties and carrier concentrations for each colour has been discussed and state-of-the-art efficiencies of 0.7% in the green (Ref. 7) and 15% in the red (Ref. 8), reported.

Red E.L. is generated within a few microns of the junction on the p-side. Junction carrier concentrations of $\sim 10^{18} cm^{-3}$, on the n-side and $\sim 5 \times 10^{17} cm^{-3}$ on the p- are currently found to be optimum values. Either S or Te is normally selected as the n-type dopant, and the favoured p-type dopant is Zn. Maximum oxygen concentrations of $1 - 2 \times 10^{17} cm^{-3}$ (Ref. 9) are achievable in the p-region via Ga_2O_3 additions to the melt. Emission occurs via the recombination of excitons bound to Zn/O pairs. Enhancement of the red emission occurs during annealing processes when the formation of Zn/O nearest neighbour pairs is maximized.

The preparation of efficient green-emitting double-L.P.E. junctions requires a different set of junction criteria. In these structures, emission takes place close to each side of the junction and originates from exciton recombination at nitrogen atoms substituted on isoelectronic phosphorus sites. Reported optimum carrier concentrations are, on the n-side, $(1-2) \times 10^{17} cm^{-3}$ and on the p-side $(5-10) \times 10^{17} cm^{-3}$ with nitrogen on each side of the junction to a level $1 \times 10^{19} cm^{-3}$ (Ref. 10). This result was based on the attainment of maximum carrier lifetimes in n- and p- material.†

It would therefore appear that for single junction red/green emitting structures, compromises may have to be made between the conflicting requirements for efficient red or green emitting material.

3. Preparation and Properties of L.P.E. p-n Junctions

The 3 general methods for the preparation of L.P.E. layers and p-n junctions are broadly classified under the headings: (a) tipping (b) dipping and (c) sliding.

The bulk of the work reported here has been carried out by the tipping method in sealed quartz ampoules. Latterly, the dipping method, in an open-flow system, has yielded a superior and more controllable method of preparing nitrogen doped n-layers. Growth runs have also been completed using the sliding method. This method has been shown to give highest green efficiencies reported to date (Ref. 7).

---

† Recent work on green devices (Ref. 11) has indicated different optimum carrier concentrations of $10^{18} cm^{-3}$ on the n-side of the junction and $3 \times 10^{17} cm^{-3}$ on the p-side. These values are more compatible with the levels normally used for red-emitting devices.

For n-type epi-layers grown at BCL, the sliding technique has given the highest P.L. efficiency values; typical efficiencies from tipping and dipping methods were 35% and 75% of these values respectively.

A. 'Tipped' n-Layers - The equipment used closely corresponds to that originally described by Shih et al. (Ref. 12). A 2 1/2" bore tipping furnace with a 5" flat zone controlled to $\pm 1°C$ was utilized. 3" long growth ampoules were made from 35mm I.D. silica with an internal plug for sealing-off purposes. Substrates were all (111) oriented L.E.C. GaP of maximum diameter 28mm. Boats were either high-purity carbon or quartz. All melt constituents were at least five 9's purity and were monitored by mass spectrographic analysis.

L.P.E. growths have been carried out on (111)B surfaces of L.E.C. GaP substrates, either S or Te doped. Wafers of original thicknesses .010" or .013" were prepared for growth by a combination of mechanical polishing with 1μ Al_2O_3 followed by chemical etching with aqua regia, HCl/H_2O_2 or Br_2/meth. X-ray diffraction topography† has been used to determine the effectiveness of surface preparation procedures and also the quality of substrates from different ingots. Surfaces produced by lapping with 5μ Al_2O_3 followed by a chemical etch in 4:1 HCl/H_2O_2 for 60 secs. (etch rate 1μ/sec.) have shown no evidence of work damage. Similarly, polished surfaces etched with the same etch for 30 secs. were damage free. Dislocation densities were measured on scanning x-ray topographs of {333} reflections at positions approximately midway between the edge and centre of the slice and compared to those obtained from chemically-mechanically polished (bromine/methanol) slices etched in 8ml H_2O, 10mg $AgNO_3$, 6ml HNO_3 and 4ml HF for 5 mins. at 70°C. Those determined by the x-ray method were in the range 1-3 x $10^4 cm^{-2}$, the chemical method giving values approximately 2-5 times higher. The majority of slices received from commercial suppliers showed no evidence of grain boundaries and none were found to contain precipitates greater than 10μ diameter, which is the probable maximum resolution of the method.

In a typical growth run a maximum tipping temperature of 1070°C was employed, and melt saturation was ensured by utilizing a 10% excess of GaP. Nitrogen was added in the form of GaN, P_3N_5 and/or NH_3, with Te as the n-type dopant. Ampoules were sealed under vacuum or ∿ 1/3 atm pure argon.

Prior to tipping, 20-30 minutes was allowed for melt equilibration. Cooling of the melt was carried out according to two schedules.

(a) At rates from 1°-8°C per min., terminating the growth at 900°C by rapid cooling of the ampoule.

(b) A melt-back cycle as described by Saul, (Ref. 13) formulated to minimize dislocations in the grown layer. Such a cycle employed a melt cool-down to 850°C followed by raising the temperature to 1000°C and a further slow cool-down to 850°C.

† X-ray topographic analyses were provided by Dr.A. Brown, Communications Research Centre, Ottawa.

In both methods, the gallium melt was retained on the surface of the substrate during quenching resulting in 1-3 mil thick epi-layers with a typical surface as shown in Figure 6. These surfaces are characteristically tiled as shown if the melt is cooled down rapidly from ~900°C. They differ both in appearance and electrical properties from those in which the gallium is decanted from the substrate at the end of the growth cycle. The last material to grow from the rapidly cooled solution is dendritic and contains higher Te concentrations than the normal n-layer due to the build up of Te in the melt adjacent to the growth interface. This was established by surface breakdown voltage measurements and surface Schottky barrier capacitance analysis on 'as-grown' surfaces containing $\sim 3 \times 10^{18}$ carriers cm^{-3}. There is an abrupt change to values close to that of the bulk n-layer ($\sim 10^{17}$) after removal of ~2μ by etching.

Photoluminescent efficiency measurements of these surfaces, both as-grown and after shallow etching are identical, as the 4880Å argon laser line penetrates about 10μ into the epitaxial layer and hence gives a bulk rather than surface evaluation.

Photoluminescence spectra were measured both at room temperature and 77°K in the following manner. The sample was excited with an argon-ion laser and the generated luminescence was focused through a CS3-68 filter (to absorb scattered laser radiation) into the entrance slit of a 0.3m scanning monochromator. Various photomultiplier tube detectors were employed to measure the luminescence over the visible and near infra-red region of the spectrum (S-20 for 5000-7000Å, RCA C31025 for 7000-8800Å, S-1 for 8000-10,000Å). All samples were prepared with an absorbing back surface, in the form of an evaporated and sintered Au (1.0%) Be film, to eliminate multiple pass photons (Ref. 14).

Figure 7 shows the photoluminescence spectra at 77°K of tipped n-layers and, for comparison, of an n-type GaP substrate and a dipped n-layer from 2.10eV to 2.34eV. Spectra are corrected for system response. The various nitrogen atom- and nitrogen atom- pair-related peaks and their phonon replicas are indicated. From the relative heights of the A, A-O, and NN peaks at the excitation intensity used, estimated nitrogen concentrations were calculated and are indicated in the figure. Although the tipped layer was grown with sufficient GaN in the melt to theoretically give the same nitrogen concentration as found in the dipped layer, these spectra indicate that the nitrogen was not incorporated in the tipped layer (Auger-related processes are minimized at low temperatures, and no other significant defect-related peaks were observed). These results highlight the distinct variations in N incorporation levels between the open and sealed L.P.E. systems.

Figure 8 shows the room temperature and liquid nitrogen temperature near infra-red photoluminescence spectra of a GaP substrate doped to $5 \times 10^{17} cm^{-3}$ with tellurium. These spectra are uncorrected, but the RCA C31025 photomultiplier has a relatively flat response in the region measured (at 77°K). We believe the higher energy 77°K peak (at 1.72eV (7215Å) is associated with Ga vacancies (Ref. 7, 14) and that the lower energy peak (at 1.48eV (8400Å) is associated with Si-O complexes (Ref. 15, 16). These peaks were not detected in epitaxial n-layers, which is reassuring, especially as the Si-O complex has been identified as a major contributor to reduced minority carrier lifetimes and diffusion lengths (Ref. 15).

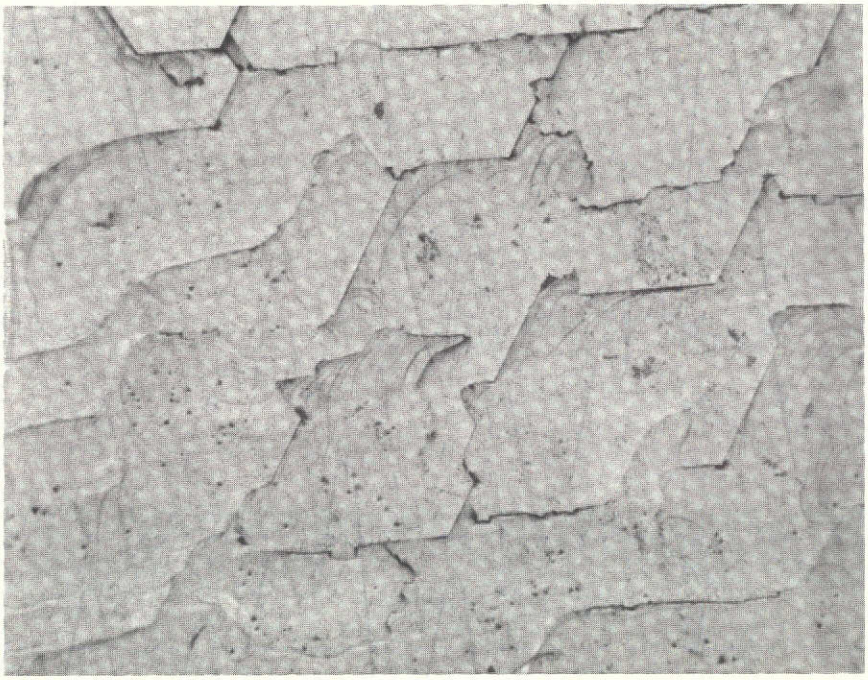

Figure 6 Typical Tipped n-Surface
- Melt Retained During Cool Down
(Magnification X 125)

This page is reproduced at the back of the report by a different reproduction method to provide better detail.

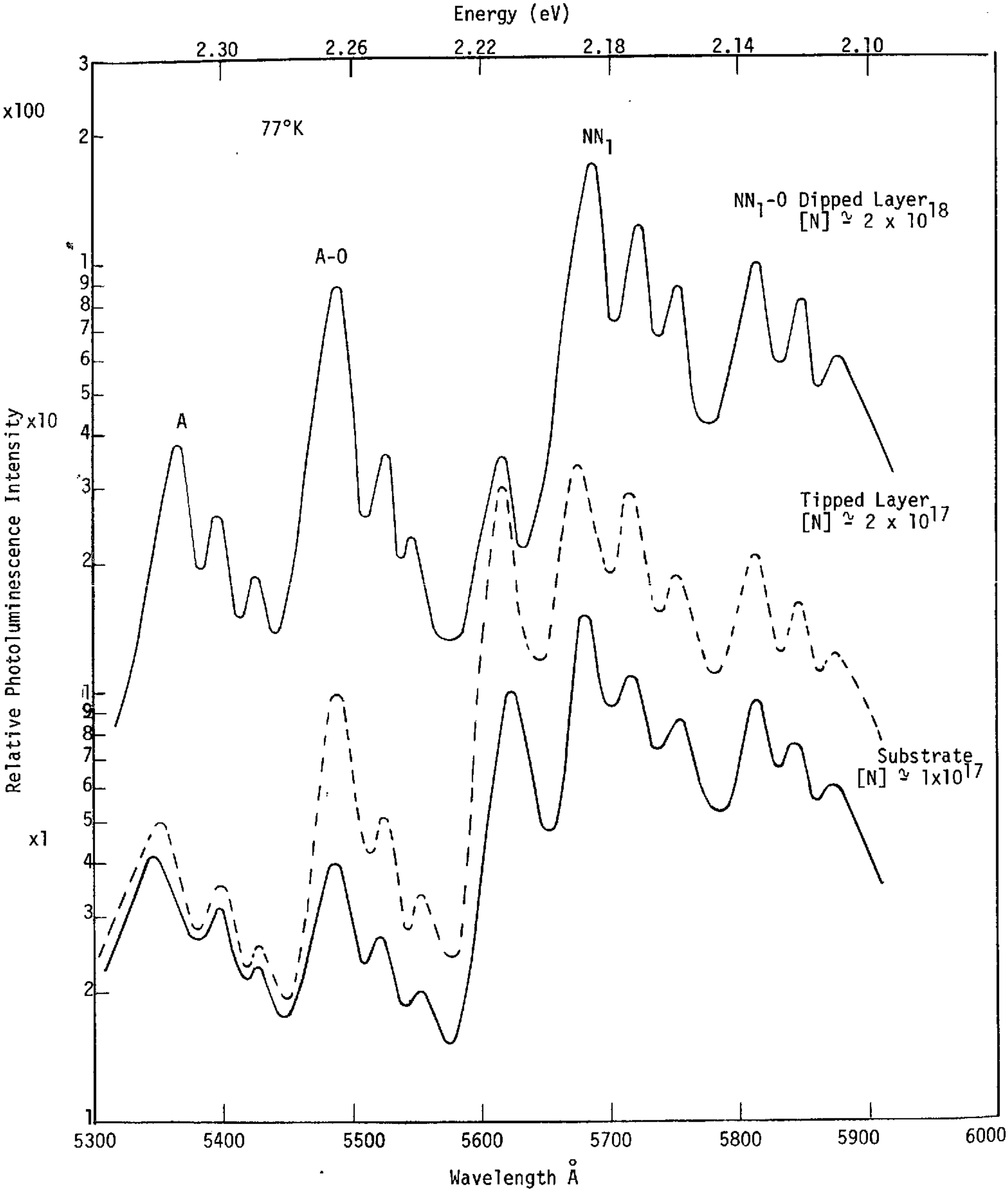

Figure 7 Low Temperature Photoluminescence of GaP LEC Substrate And Liquid-Phase-Epitaxial Layers

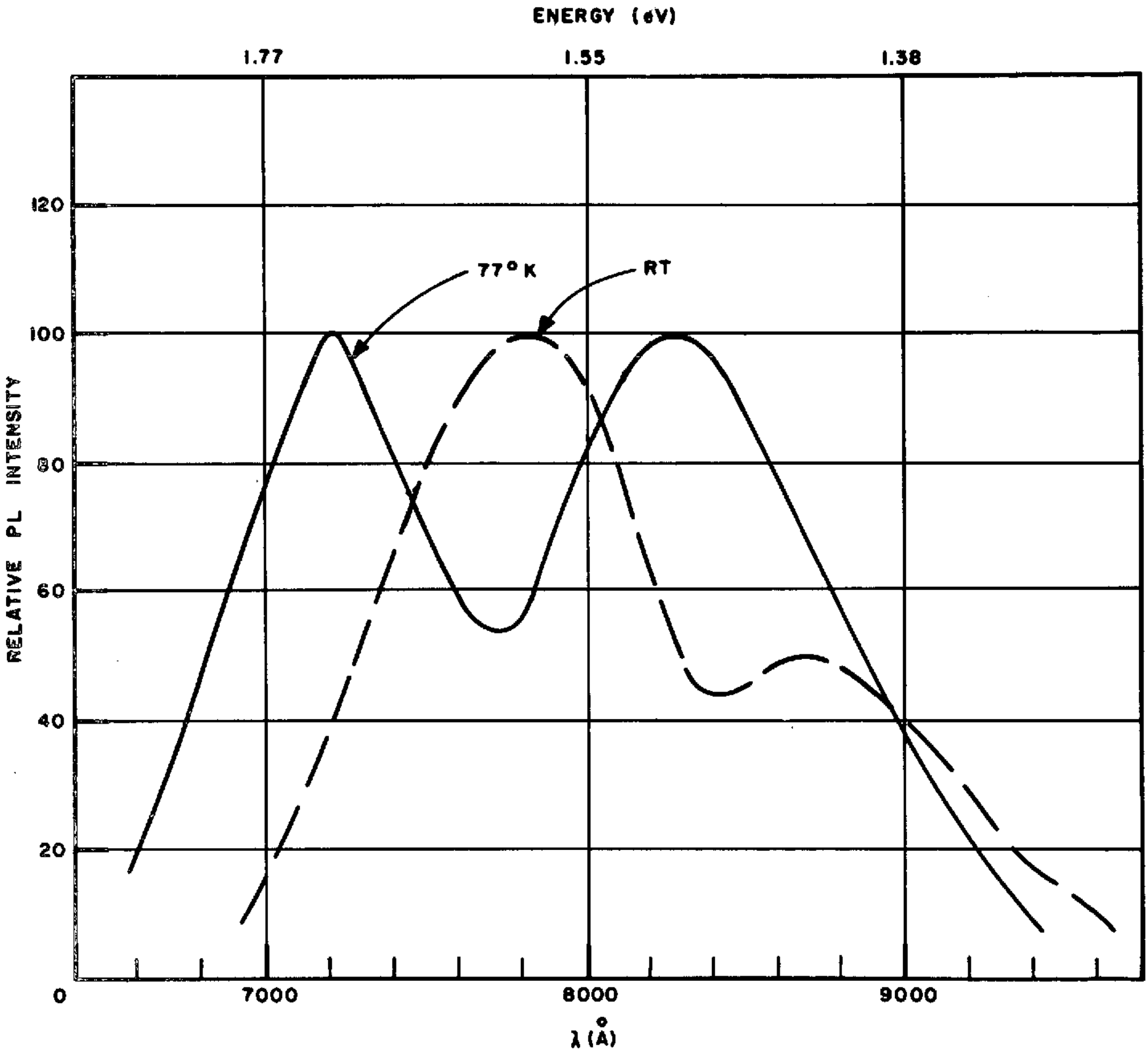

Figure 8 Infra-Red Photoluminescence Spectra Of Te-Doped GaP Substrate

To further ensure that oxygen contamination was not significant, epitaxial layers and substrates were diffused with zinc, annealed for several hours at 500°C, and the photoluminescence due to excitation recombination at Zn-O pairs measured. Red P.L. was very weak in all samples processed in this way, (red P.L. efficiency <.01%), and the diffused epitaxial layers showed less red intensity than the diffused substrates; thus, we have an indication that oxygen concentration is at a low level, although we cannot rule out the possibility of a significant Si-O complex concentration.

The aim in the growth of n-layers has been to incorporate a maximum concentration of nitrogen and, using the technique described above, to monitor the n-carrier concentration as a function of P.L. efficiency, and correlate with the green component in the final red/green device. Nitrogen additions are limited to levels of approximately $10^{19}cm^{-3}$, by the appearance of characteristic hexagonal growth defects on the surface. The solubility of nitrogen in solution-grown GaP increases with the growth temperature (Ref. 17) and some compromise must be made between maximizing the nitrogen content and introducing non-radiative and lifetime-killing (e.g. Si and O) impurities from containers etc. at the higher temperatures used.

The level of nitrogen introduced into the epi-layer is influenced by the pre-growth equilibration procedure, rate of growth, maximum temperature, and temperature span. In the present work the maximum growth temperature was 1070°C. We have observed little difference in N content for layers grown from starting temperature 1000°C to 1070°C; however, superior P.L. and E.L. efficiencies were obtained at higher growth temperatures.

Measurements of P.L. intensity vs cooling rate from 1000°C indicate that a poorer surface quality and lower nitrogen concentration is obtained at 1°C/min.; however, at 8°C/min. the Te gradient through the n-layer becomes quite large, and the concentration is erratic near the surface (Ref. 18). Hence, as a compromise we have used a cooling rate of 5°C/min. The attainment of maximum concentrations of nitrogen in the surface of grown layers is important because this is the region in which the p-n junction is ultimately formed.

The incorporation of nitrogen into n-material grown by the tipping method has led to erratic results. In the latter stages of the program, the method was discontinued and replaced by the dipping method which was shown to produce more consistent results. A summation of our results and conclusions on the tipping method of introducing nitrogen are as follows:

(a) Hexagonal defects in the grown crystal are not necessarily the direct result of too high a nitrogen concentration. They may also be due to spurious growth nucleations caused by GaN particles. Evidence for this was obtained from several experiments with a carbon boat design in which one substrate was situated above, and spaced apart,from another. The melt rolled over the bottom slice first and then covered the upper slice. The upper grown layer was generally quite smooth even though the bottom layer showed evidence of nitrogen hillocks. We believe that GaN particles (from undissolved GaN additions or melts oversaturated with nitrogen via NH_3 additions) are effectively filtered from the melt as it moves over the surface of the lower substrate. The photoluminescence intensity was lower for bottom slices than for top slices.

(b) A carbon boat designed to skim the melt free of any particulate matter produced smooth epi layers. In these experiments, four times the nitrogen additions could be made as for the boat in (a).

(c) Nitrogen doping via GaN or NH_3 showed the same inconsistency in P.L. efficiency of grown epi layers, i.e. the effect is not related to one particular technique of nitrogen incorporation.

The best and most uniformly nitrogen doped layers were produced in boats as described in (a) where the two slices were covered with melts of constant thickness. Nitrogen additions to the melt were controlled such that under-saturated conditions were obtained and free GaN absent.

In Figure 9 is shown the effect of GaN concentration in the n-layer melt on photoluminescence intensity; results are similar to those found by Wight et al. (Ref. 11). The plateau at higher concentrations of GaN is due to the onset of disturbed layer morphology.

From the P.L. spectrum we have observed a 50% decrease in nitrogen concentration from the epitaxial surface to the substrate interface on angle lapped surfaces. The Te concentration decreases by a factor of 2-3 over the same region for the cooling rate employed (5°C/min.). The photoluminescence P.L. decrease is due both to a decreasing nitrogen concentration toward the substrate and the decreasing ionized donor concentration.

Maximum red/green efficiencies were obtained from n-layers with the following characteristics: Excess donor concentration at the junction (N_D-N_A) $\simeq$ (7.5 - 10) x $10^{16}cm^{-3}$; nitrogen doping level $\simeq$ $10^{18}cm^{-3}$.

B. 'Dipped' n-Layers - The preparation of n-layers by the process of vertical dipping in an open flow, all-quartz system has given more control over the P.L. efficiencies than the tipping program.

Brief details of the equipment are as follows: The main reaction vessel consisted of a 70mm I.D. quartz tube closed with a flat base at one end and provided with spherical socket joint at the other. A gas inlet tube sealed near the top passed to the bottom of the tube. A ball socket joint assembly carrying a gas inlet port and 2 lead-through seals completed the vessel. Flat-bottomed quartz crucibles contained the melt, the substrates being held in horizontal quartz shelves at the end of a dipping tube. The gas system consisted of a source of Pd/Ag-diffused H_2, argon purified by passing over titanium sponge at 800°C, and 2% NH_3 in nitrogen. The gas distribution system was rigorously tested with a mass spectrometer leak detector. A vertical furnace with a 6" flat temperature zone was used to heat the crucible. The essential differences between the techniques of dipping and tipping are:

(a) In the dipping system substrates are held outside the furnace during melt warm up and equilibration. Thus they can be inserted and withdrawn from the melt at will and layers thereby grown over restricted temperature intervals. In addition, the melt may be decanted from the surface of the wafers at the termination of growth.

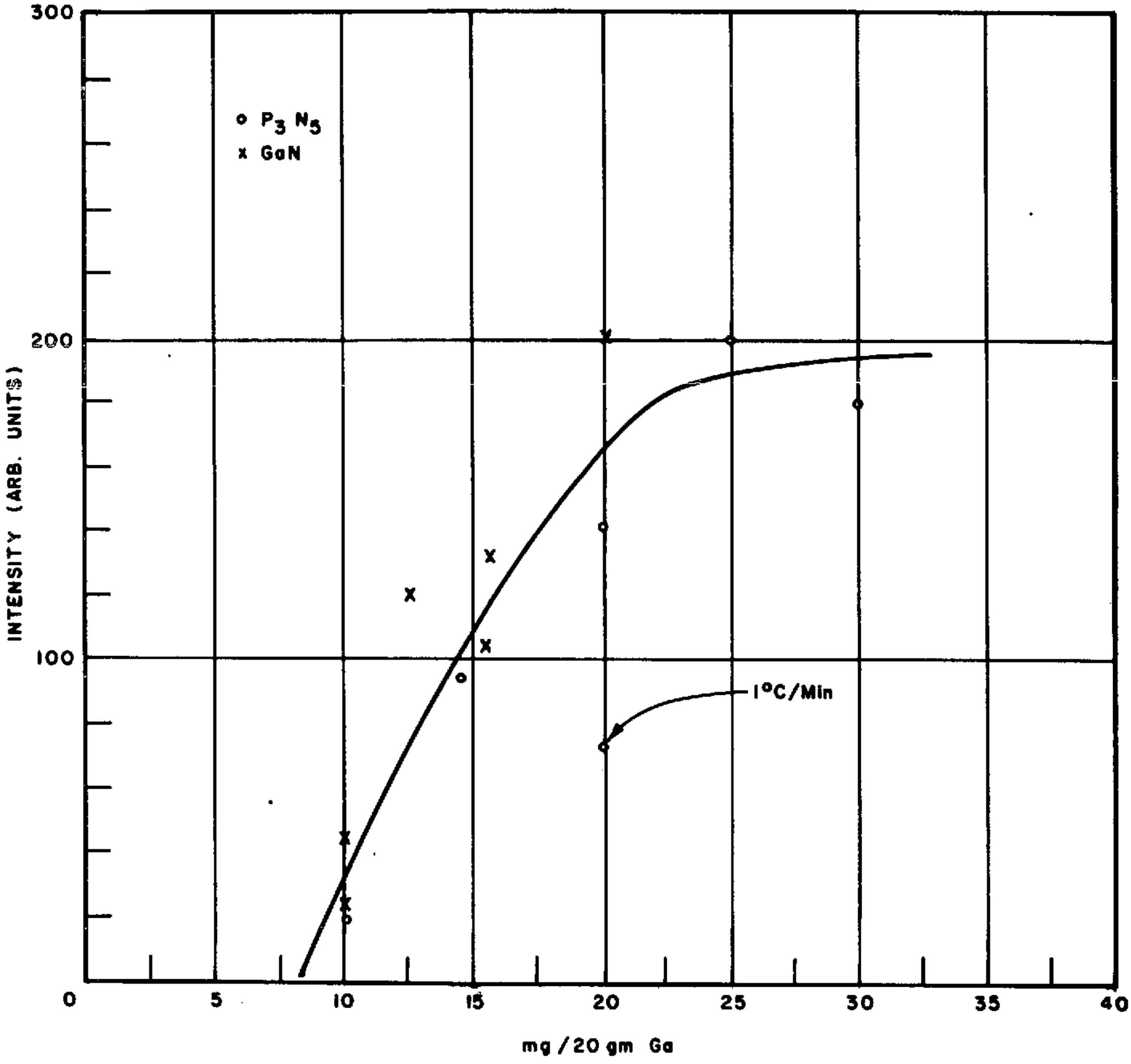

Figure 9 P.L. Intensity As A Function Of Nitrogen Addition To The Melt (Layers Grown From 1055°C, 5°C/Min. Cooling Rate)

(a) Tipped n-Layers Doped From A GaN Source

(b) Dipped n-Layers Doped From A P_3N_5 Source

(b) In the open flow technique, the stoichiometry of the grown crystal can be controlled by modifying the vapor species in the system, a factor which may influence the kinetics of both defect formation and nitrogen incorporation.

Layers with the highest reproducible P.L. efficiency were obtained by using P_3N_5 or GaN as the nitrogen source. Consistent with our findings on tipped n-layers, the use of NH_3 induced layer defects attributed to GaN particles nucleating spurious surface growths. With GaN or P_3N_5 additions a well-fitting quartz float could be used on top of the melt. On dipping the substrates, this effectively held down GaN particles due to any excess N in the melt and produced very smooth surfaces with high relative P.L. efficiency (Figure 10). Figure 9 also shows the resultant photoluminescence intensity as a function of P_3N_5 content in the melt In a given run the emission efficiencies varied by $\pm 10\%$ across a wafer and $\pm 20\%$ wafer-to-wafer. This compares favourably with results from the tipping program, where wider variations were encountered.

Melt temperatures between 900°-1070° have been used, and, as with tipped layers, generally higher P.L. was obtained at higher temperatures. Withdrawal of the substrates has been carried out to ensure melt removal from the surface of the grown layer. In Figure 11 a surface is shown where this has occurred and on the same substrate a portion where the Ga melt remained in contact during cool-down. Reverse breakdown voltage measurements indicate surface concentrations of $\simeq 5 \times 10^{17}$ atoms cm^{-3} on the clean surface and $\simeq 3 \times 10^{18} cm^{-3}$ on the rest. A doping profile through the n-layer after removal of the high concentration surface is shown in Figure 12.

In a quartz substrate holding system conditions for constitutional supercooling may be present due to the minimal temperature gradient imposed across the thickness of the slice. Several experiments were made using a graphite slice holder with a thick substrate platform designed to hold a slice vertically and to provide an improved ΔT (Ref. 19). In these experiments no significant improvement was noted in either layer quality or P.L. efficiency.

C. <u>Use of a Sliding-System for n-Layer Growth</u> - Liquid epitaxial growth systems based on variants of the sliding technique (Ref. 20) have been widely utilized in application to GaAs and GaAlAs device structures; the highest efficiency green GaP devices reported to date have been prepared in apparatus of this type (Ref. 7).

In the present program the sliding technique has not been investigated extensively, however, as indicated previously, the photoluminescence characteristics of n-layers prepared using this procedure were noticeably improved in comparison with the dipping method. The technique investigated involved the use of a pyrolytic graphite slider assembly mounted in an open-flow system; the carrier gas was Pd-purified hydrogen and NH_3 was used as the nitrogen source. The n-type dopant, Te, was added directly to the melt; growth was normally initiated at 1020°C, and the system cooled over a 20°C-40°C temperature span at 1°C/min., resulting in epi-layers of thickness 2 mils.

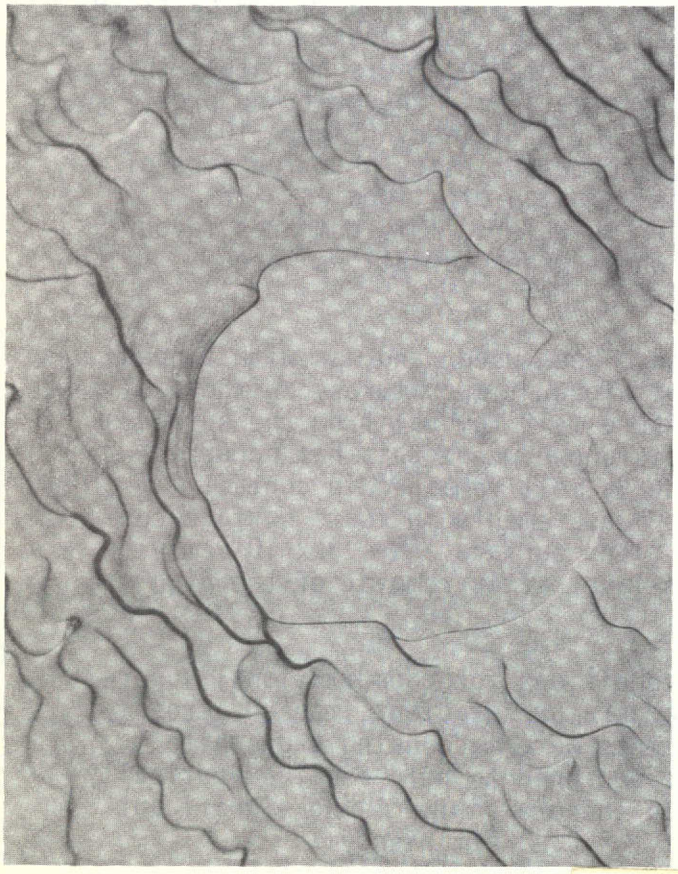

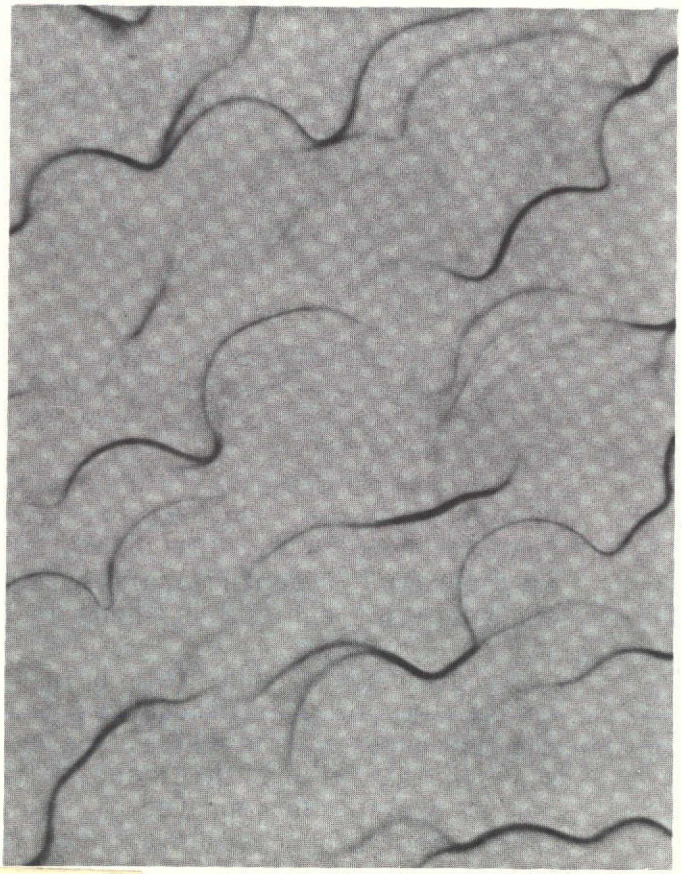

This page is reproduced at the back of the report by a different reproduction method to provide better detail.

Typical Featureless Area On Dipped GaP N-Layer With Melt Decanted (Magnification X 60)

Dipped GaP N-Layer Melt Decanted At End Of Growth Cycle (Magnification X 125)

Figure 10 Surface Morphology of GaP LPE N-Layers Prepared In A Dipping System

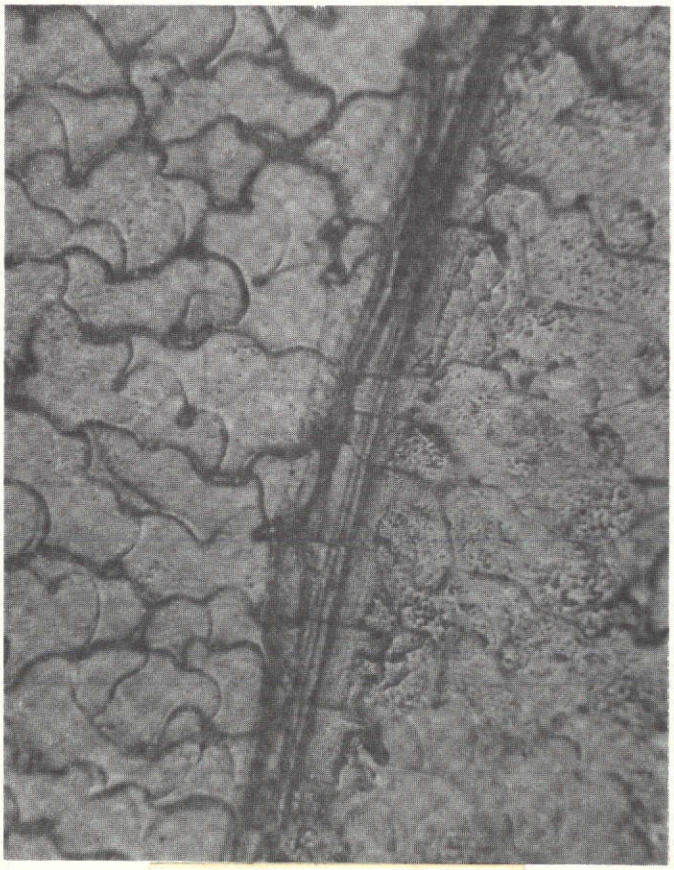

Figure 11 Surface Morphology Of A GaP n-Layer Showing Effect Of Draining Ga Off Substrate On Removal From The Melt In A Dipping System. Left Side Of Photomicrograph Shows The Area Where Ga Drained Off The Surface

(Magnification X 60)

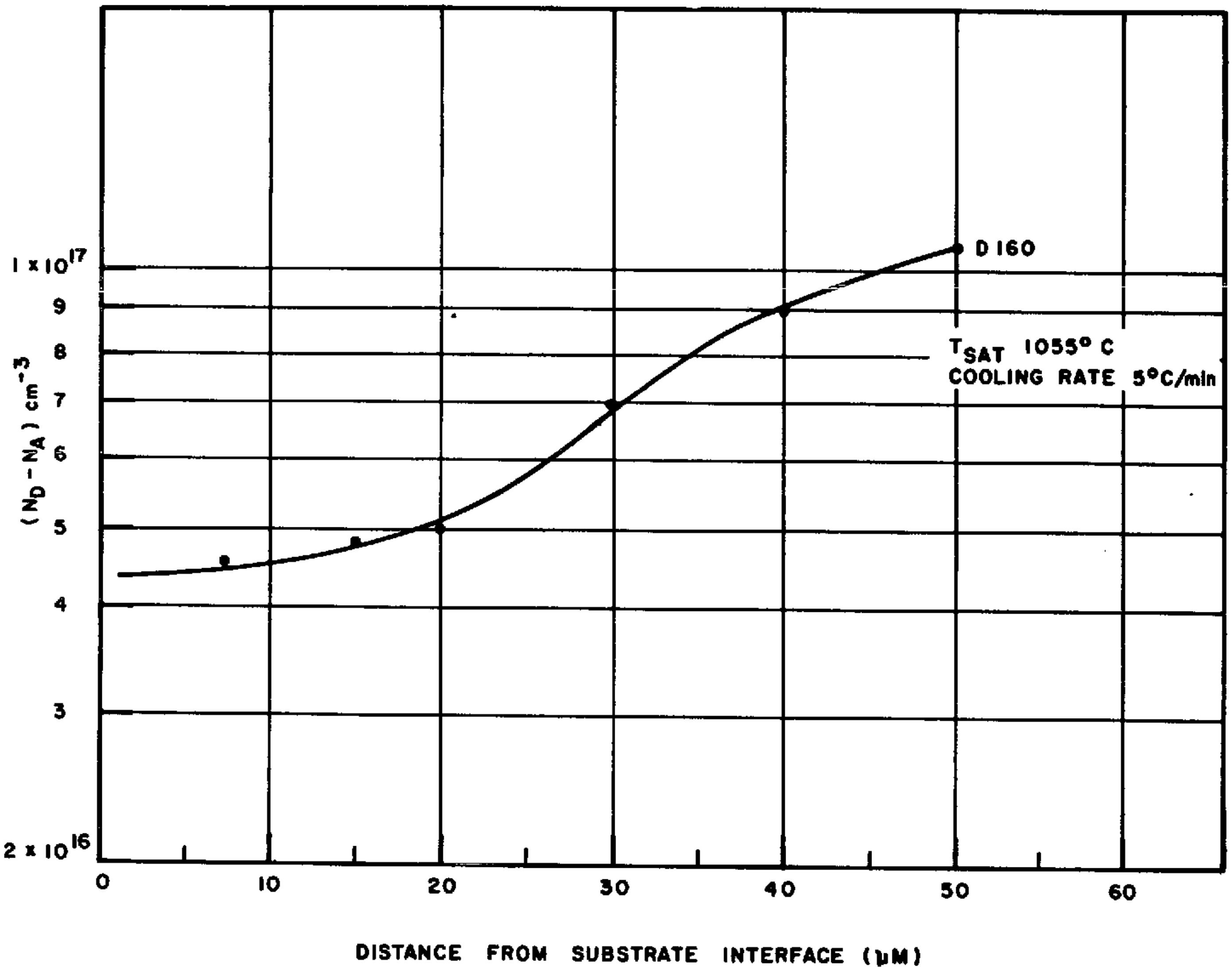

Figure 12 Doping Profile Of Tellurium-Doped Epitaxial n-Layer Grown In A Dipping System

D. 'Tipped' p-Layers - Conventional tipping techniques were found to provide a reliable and convenient method of preparing Zn-O doped p-layers for red/green device fabrication. An advantage of sealed ampoule p-growths lies in the fact that a high measure of control can be maintained over the partial pressure of Zn and thereby its final concentration in the epi-layer.

For tipped n-layers, the removal by chemical etching of the high Te content material, referred to in the last section, has been monitored with changes in surface reverse-breakdown voltage measurements. Approximately 5μ deep etches were employed. Mass spectrographic analysis of the surfaces resulting after treatment with HCl/H_2O_2 etches, for example, indicated the presence of up to 1700ppm (atomic) of oxygen as compared to 20ppm in the bulk of the layer. Oxidized surfaces have been reported (Ref. 21) to produce poor quality epi-layers resulting from initial island type growth and subsequent Ga entrainment. For preparing n-surfaces, non-aqueous etches, such as 10% bromine / methanol, have been preferred.

For dipped n-layers, where the process of gallium melt decantation has been successful, no surface treatment has been found necessary prior to the p-layer growth. Growth of p-type layers was carried out from a maximum melt temperature of 1070°C. Melts containing excess GaP and Ga_2O_3 were cooled at 10°C/min., the capsule being subsequently quenched from 900°C to room temperature to minimize diffusion of Zn into the n-region.

E. 'Dipped' p-Layers - The dipping system described previously was investigated in application to p-layer growth. The growth of Zn-doped p-layers in an open-flow dipping system leads to losses in the Zn component due to its relatively high vapour pressure at the growth temperature used. As reported elsewhere (Ref. 19), the use of a well-fitting float on top of the melt significantly reduces the loss and also provides a means of filtering the melt as the substrate is dipped. In comparison with results obtained for dipped n-layers, the characteristics of dipped p-layers, evaluated in terms of P.L. intensity, P.L. uniformity, doping gradient and uniformity, and layer morphology, were not found to be superior to similar layers grown in a tipping system.

The dipping system was also used for the preparation of nitrogen doped p-layers, in order to compare the performance of red/green devices with green-emitting devices having similar n- and p-type doping levels. No modifications were made to the growth schedule. The nitrogen doping source was again P_3N_5. Photoluminescence efficiency levels were similar to those obtained for nitrogen-doped n-layers.

F. "In-Situ Junctions"- The growth of 'in-situ' junctions has been achieved by stabilizing the temperature after the growth of a thin n-layer and overdoping the melt with Zn. To date, junctions prepared in this way have not exhibited device efficiencies equal to double L.P.E. procedures.

4. Annealing Procedures

Post-growth annealing cycles are widely utilized to enhance the emission efficiency of red and green-emitting GaP devices (Ref. 22, 23). Such procedures can also be used effectively to modify and improve the performance of red/green devices. Attainable improvements in the green are found to be less pronounced than for the red. For the device structures used in the present work, the maximum improvement in green efficiency resulting from short-term annealing at temperatures in the 600-700°C range was a factor of two, with a mean value considerably lower and closer to 30%. For the red recombination, extended annealing for periods of 16 hrs. at 500°C resulted in improvements of up to an order of magnitude in emission efficiency. The green component was found to increase by up to 15% with this annealing schedule. The outcome of these annealing procedures were found to be one of the less predictable aspects of red/green material processing. This situation reflects variations in incorporated impurity and defect complex levels and the distribution of Zn-O recombination centers. In general, a non-linear dependence was found between the period of the annealing schedule and the resultant improvement in red emission efficiency - the major change in efficiency occurred during the early stages of the anneal; however, the results at this point showed more scatter than at completion of the extended anneal. Annealing results were not markedly influenced by the ambient conditions, but use of a Ga melt was preferred.

It was therefore found possible to tailor the final performance characteristics of red/green material to a certain degree, by evaluating the as-grown performance of the material and selecting an appropriate annealing schedule to achieve an end result compatible with the display configuration (element size), anticipated drive conditions, and required brightness level. Obviously, this infers that for as-grown material the green component will dominate the emission spectrum.

5. Selected Material Characteristics

It was indicated previously that the selection of processing procedures for red/green device structures involves a compromise in terms of injection ratios and recombination center distribution between values considered optimum for an efficient red device on the one hand and an efficient green device on the other.

The composite red/green device structure selected for the present application was as follows:

n-material dopants	Te $7.5 - 10 \times 10^{16} cm^{-3}$
	N $\sim 10^{18} cm^{-3}$
p-material dopants	Zn $4 - 6 \times 10^{17} cm^{-3}$
	O $\simeq 10^{17} cm^{-3}$

Post-growth anneal-12 hr. at 500°C

Efficiency values for header-mounted devices were 0.75 - 1.5% for the red component at current densities of $5A/cm^2$, and 0.01 to 0.02% for the green component at a current density of $250A/cm^2$. All efficiency measurements were made on epoxy-encapsulated header-mounted devices. No attempt was made to maximize emission efficiency by optimizing the device geometry.

To obtain some indication of the comparative performance of pure red and green devices having the same injection characteristics as the device structure referred to above, two sets of experiments were conducted. First, nitrogen was eliminated from the n-layer and the device subjected to an extended 500°C annealing cycle. Subsequently, device structures were fabricated in which oxygen was eliminated from the p-layer and nitrogen incorporated on both sides of the junction. Efficiency measurements showed an increase in red efficiency to 2.5% accompanied by an order of magnitude reduction in the high current density green efficiency. For the green device, the efficiency of the red component was reduced to the 10^{-2}% range accompanied by an increase in the $250A/cm^2$ green component to 0.08%.

IV DISPLAY PROCESSING AND FABRICATION

1. Design Considerations

As discussed previously, the recommended approach to fabricating an information display capable of generating full alphanumeric information in a multicolor format is to use a single-junction GaP monolithic X-Y addressable 5 x 7 format.

Several factors must be considered in the design of the 5 x 7 array that is ultimately used. These factors include:

- device geometry
- element density and addressing techniques
- internal reflections and scatter
- current-carrying capacity
- reliability
- filtering

A. Geometry - The minimum character dimensions were established in the original work statement as 0.125 x .090 inches. The dimensions of each element is a compromise which involves consideration of both the clarity of the generated symbol and the drive current requirements necessary to achieve the multicolor presentation. The superlinear dependence of the green-component emission intensity on current density infers that the smaller the junction area, the brighter the device will appear when operated in the green mode. However, since the red component saturates at relatively low current densities, the brightness of this component is dictated by the absolute efficiency and saturation characteristics of the red recombination. Therefore, the increase in emission intensity which can be achieved by raising the current density is limited and may involve a sacrifice in color clarity. However, by reducing element size, any selected brightness level considered acceptable in terms of color definition can be obtained at lower operating currents. For given material efficiency, the element size must therefore be selected to produce a brightness match between the unsaturated red component achieved at low current densities and the high current density green component. If the active junction area is too large, the current required to achieve sufficient green intensity will be excessive, while for fixed operating current, too small an element may result in a change in visual hue of the red component.

B. Element Density and Addressing Techniques - Addressing techniques and material performance characteristics are important criteria in determining the maximum element density of a multi-color display. In this connection, the critical factor is the saturation characteristics of the red emission band. For material of given efficiency and specified brightness level, the maximum number of elements is determined by the peak current which can be applied to one element of a scanned array before the shift in visual hue away from a distinct red coloration becomes unacceptable.

These considerations are highly significant in the design of large area displays, but do not impose a severe restriction for 35 element arrays as used in the present application.

C. Scatter - The red and green emission band associated with indirect radiative recombinations generated at a p-n junction in GaP are not effectively self-absorbed. Pertinent absorption data is shown below, including, for comparison, the red emission of a direct-gap $GaAs_{.6}P_{.4}$ alloy.

Material and Dopant	Emission Wavelength (Å)	Path Length in Material to Attenuate Emission by 20:1 (cm)
$GaAs_{0.6}P_{0.4}$(Te)	6500	10^{-3}
GaP (Zn, O_2)	6950	3×10^{2}
GaP (Te, N_2)	5650	2.7×10^{-1}
GaP (Te)	5550	3×10^{-1}

Fabrication techniques must therefore be chosen which artificially prevent light scatter from an activated element to its neighbouring unenergized devices. This requirement precludes the use of a number of conventional monolithic processing procedures applicable to other semiconductor devices.

To illustrate the effects of optical crosstalk between adjacent segments, measurements were made on a red/green display which had fully isolated columns and rows which were diced to a depth just below the p-n junction (Figure 13). A fiber-optic probe was used to obtain brightness measurements at selected points on the array surface and in the isolation grooves. Measurements were only made on the red component since it represents the major contribution to the scattered emission. These results highlight the requirement for either complete isolation of the emitting segments, or the incorporation of an optically isolating medium.

D. Current Density - Peak currents to switch a single junction multicolor device into the green mode is a few hundred milliamps at a low duty-cycle. The device design and packaging considerations must provide for adequate thermal dissipation as well as conductors of dimensions sufficient to accommodate these high current levels. The cathode columns may be attached directly to a circuit board or, in order to improve the heat dissipation characteristics of the package, to an intermediate ceramic substrate.

E. Reliability - Closely related to the current capacity requirement is reliability. The design must consider the reliability of the finished device in terms of the necessary drive conditions, and the environmental test schedule.

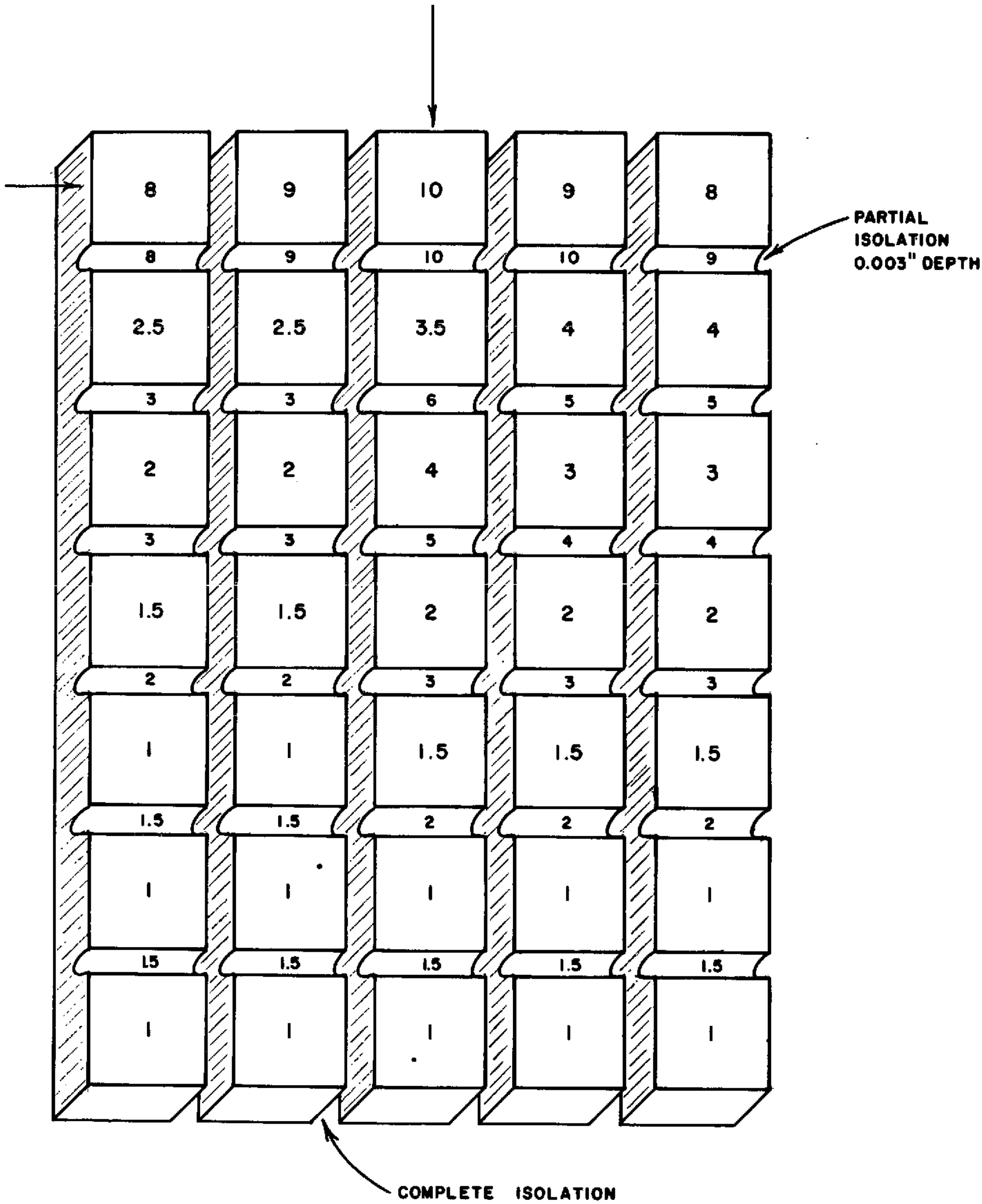

Figure 13 Relative Emission Intensity Map For A Micro-Diamond Saw Isolated Red/Green Matrix With One Element Activated. (The Addressed Element Is Indicated)

F. Filtering - The emission from a two-color device covers a wide portion of the visible spectrum. A broad band-pass filter is therefore required. In addition, it is important to minimize reflections within the package. Several materials were investigated, and a neutral-colored circularly polarizing filter was selected - the latter primarily for the purpose of minimizing surface reflections. The results of contrast measurements using this filter system are presented in Section V.

2. Fabrication

The proposed array fabrication techniques included the diffusion of 'p' impurities into 'n' type V.P.E. or L.P.E. material to form planar junctions. However, this form of device processing failed to produce material exhibiting efficiency levels sufficient to warrant further investigation. Consideration of suitable array structures was therefore restricted to double-liquid-epitaxial materials. The fabrication possibilities of this type of device are limited in the following respects:

(a) a full-surface junction is produced, necessitating mechanical, or chemical, element delineation

(b) limited choice of element size and shape

(c) a deep junction, eliminating the use of diffusion-isolation techniques

The design considerations outlined in Section 1, combined with the processing limitations expressed in the present section, must now be applied to the fabrication procedure for the final array.

In the fabrication of an X-Y addressable GaP array, the most difficult requirements to accommodate are those associated with electrical isolation of adjacent columns and the minimization of optical crosstalk. In relation to the former, diffusion isolation techniques are impractical and physical isolation procedures must be adopted. To completely eliminate crosstalk, it is necessary to introduce an opaque epoxy between adjacent segments. The grooves created during the isolation step are readily compatible with this procedure. Indeed, if diffusion isolation techniques proved practical, supplementary processing procedures might still be necessary to fully comply with the crosstalk specification.

A. Contacts - A major factor in the successful fabrication of a two-color GaP array is the contact to the semiconductor. This contact must meet several criteria. First, it must be ohmic to material which has a carrier concentration in the 1-5 x 10^{17} carriers cm^3 range.

Second, it must adhere well to the semiconductor surface and be suitable for subsequent bonding operations. Many of the gold alloys often used for GaP processing do not adhere well to oxide or nitride passivation layers. The contact material must also be compatible with photolithographic delineation techniques. Finally, it is desirable that the contact to the rear face of the display be reflecting, so that light directed away from the viewing surface will enhance the total external emission.

Contacts selected for the present application were Au(1.0%)Be for the p-contact and Au(13%)Ge for the n-contact.

Other contact systems investigated and the resistivity measurements obtained are listed below.

Material Type	Carrier Concentration $N_d(cm^{-3})$	Contact Type	Contact Resistivity ρ_c *
n	2×10^{17}	Au(13%)Ge/+Ni	8×10^{-4}
	5×10^{17}	Au(13%)Ge/+Ni	3×10^{-4}
	2×10^{17}	Ag(2%)Te/+Ni	3×10^{-3}
	2×10^{17}	Ag(13%)Ge/+Ni	3×10^{-2}
p	3×10^{17}	Al	Non-ohmic
	3×10^{17}	Au(2%)Zn	5×10^{-2}
	3×10^{17}	Au(1%)Be	2×10^{-3}

* ρ_c [Ω-cm^2] = R_c x area, where R_c is the contact resistance

B. Array Fabrication - The technique adopted to fabricate the deliverable hardware emphasizes optical and electrical isolation, as well as element dimensions, with some compromise on the truly monolithic nature of the structure.

The as-grown material was lapped on the 'n' face until a total wafer thickness of approximately .008" was obtained. A film of Au(1%)Be was evaporated over the 'p' surface, and alloyed to improve adhesion and electrical characteristics. The contact pattern was then delineated to provide a limited-area bonding pad for each device. A chemical clean-up etch was used to remove any residual alloy residue remaining on the surface in regions remote from the contact. Device efficiency was also improved by the resultant thinning of the p-layer and beveling of the emitting surface. A Au(13%)Ge contact was applied to the 'n' surface and alloyed. This contact was deposited through holes in an oxide passivation layer. The material over the passivation provides a reflecting surface which improves the external emission.

The wafer was cut on a micro-diamond saw to a depth just below the 'p' layer thereby isolating devices on a common 'n' substrate. Complete testing was performed at this stage, to determine the quality of the two color components. Acceptable 5 x 7 matrices were cut from the wafer, and mounted on a carrier board using conducting epoxy. Cathode isolation was achieved by continuing the cut completely through the material, and into the underlying carrier board.

The material was next cut to within .002" of the carrier board in the opposite direction. The cuts were then backfilled with black epoxy to eliminate optical coupling. Anode interconnections are made by ultrasonically stitch bonding across the rows and down onto the bonding pattern on the carrier board. The composite display structure is illustrated in Figure 14, and the mounting board pin configuration in Figure 15.

Finally the package was encapsulated to protect the wire bonds and fitted with a filter to give the required degree of contrast enhancement. Figure 16 shows an operating display.

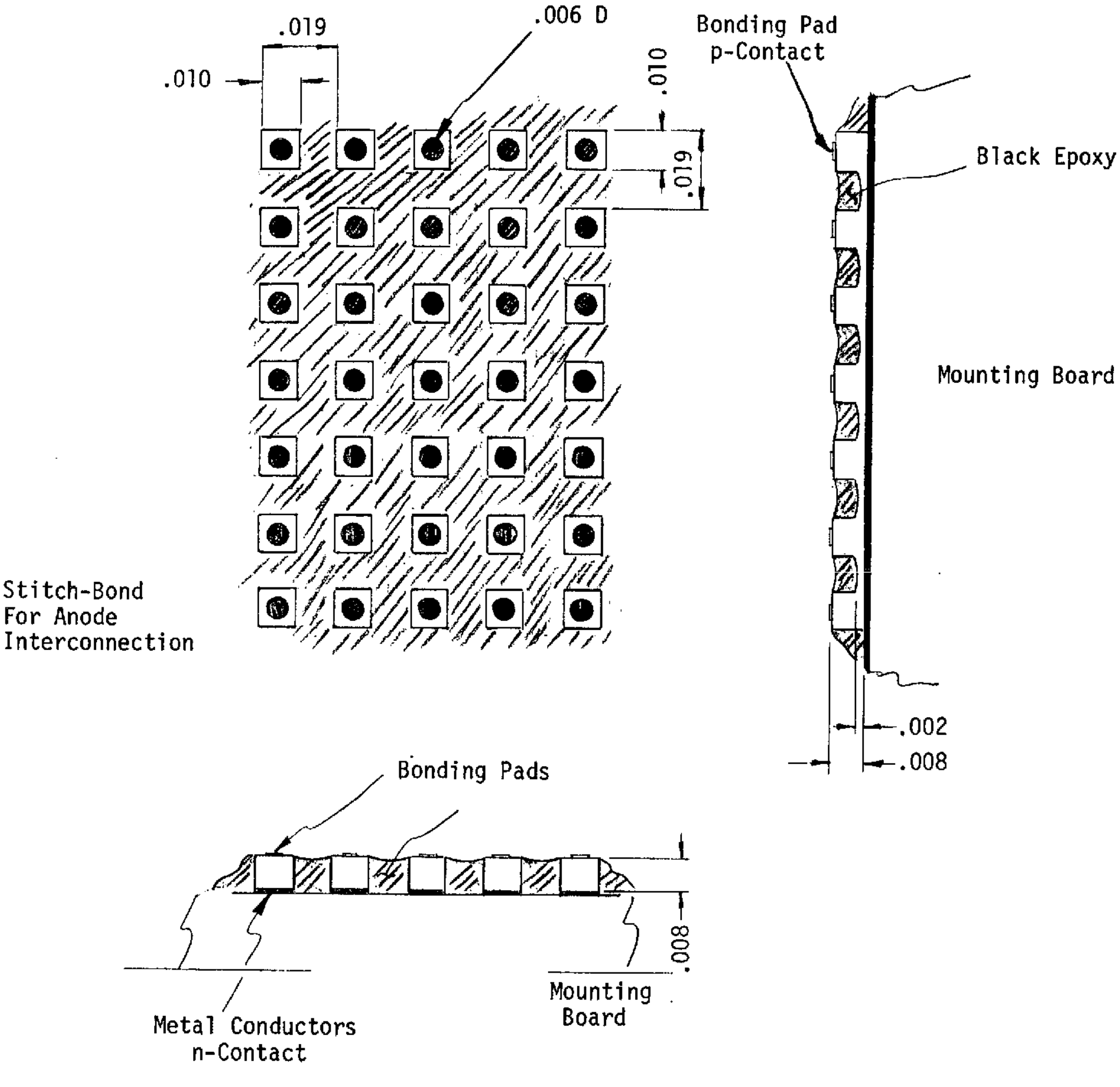

Figure 14 Structure Of A GaP 5 x 7 Alphanumeric Display

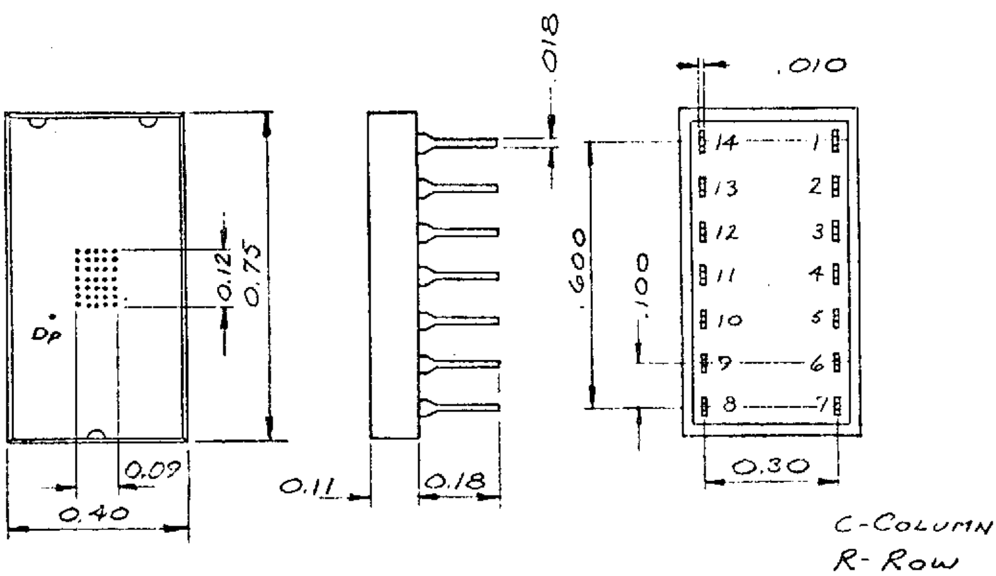

Pin	Elec Conn
1	C-2
2	R-2
3	R-4
4	R-6
5	DP-AN
6	LP-CA
7	C-1
8	C-3
9	C-5
10	R-7
11	R-5
12	R-3
13	R-1
14	C-4

Figure 15 Mounting Board P In Configuration

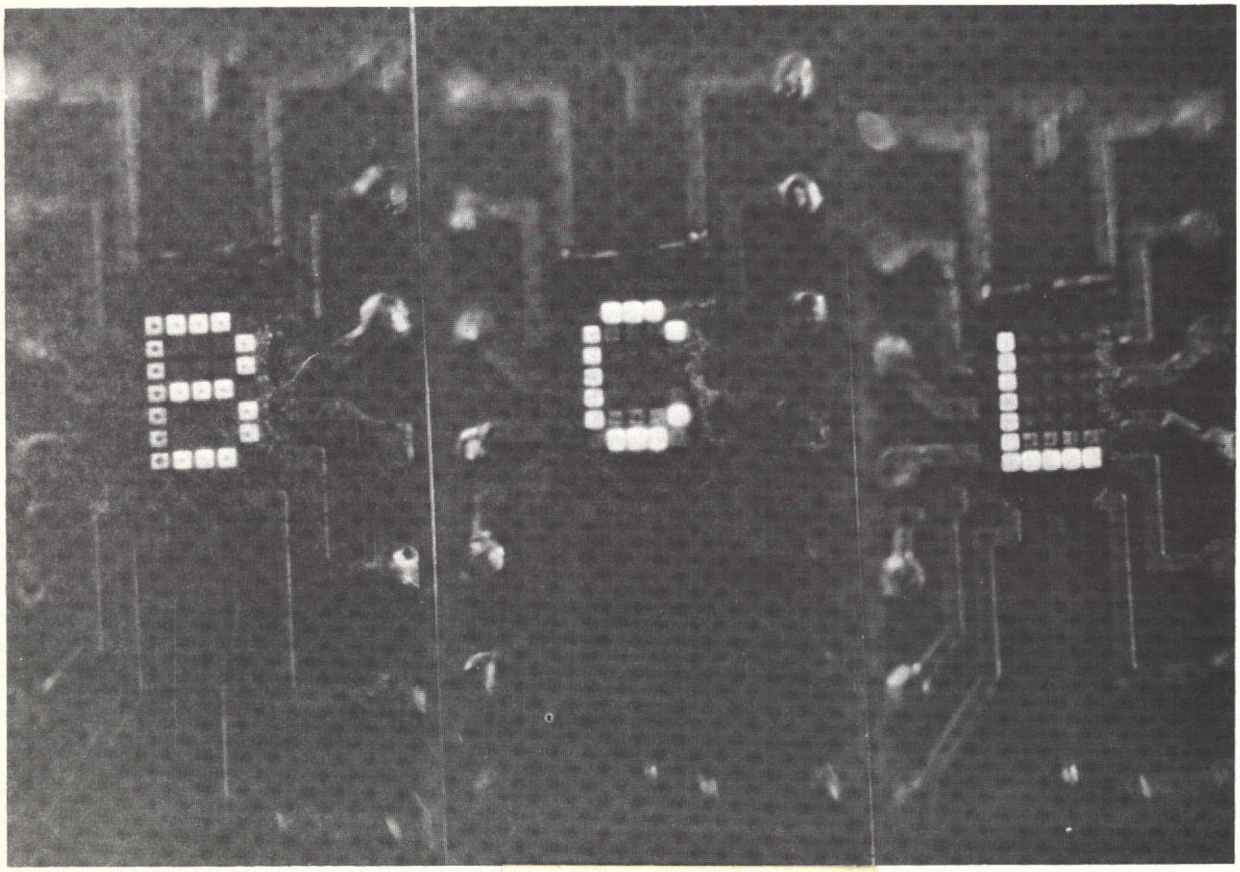

This page is reproduced at the back of the report by a different reproduction method to provide better detail.

Figure 16 Alphanumeric GaP Multicolor Display Operating In The Red-Mode. The Absence Of Optical Coupling Between Illuminated And Adjacent Segments Is Demonstrated

V DISPLAY PERFORMANCE

Generalized performance characteristics of GaP single junction red/green devices were discussed in the Introduction. This section provides details on the performance evaluation of the red/green displays supplied to NASA. The display specification and required performance tests were detailed in the program work statement.

1. Emission Spectra

Typical spectra for a red/green diode are shown in Figure 17; the electroluminescence intensity is plotted as a function of wavelength for both a typical red-mode drive condition (1KHz, 1/17 duty cycle) and a typical green-mode drive condition (1KHz, 1/200 duty cycle) at various current levels. Referring to the dominant wavelength vs peak current density shown in Section 1, the red mode drive condition quoted above corresponds to a dominant wavelength of 6200Å at 20mA peak current, the green-mode drive condition corresponds to a dominant wavelength of 5725Å at 600mA peak current.

2. Brightness Measurements

Figure 18 shows the luminance of the separate red and green components as a function of average current under an optimum red mode drive condition (d.c.) and an optimum green mode drive condition (2.3KHz, 1/160 duty cycle). The total surface luminance values under both drive conditions exceed the minimum specified value of 200-250 ft.L., (quoted brightness values are the summation of both red and green components). Under 5mA d.c. drive conditions, total element brightness is in excess of 400 ft.L. Under the red mode drive conditions of 1KHz, 1/7 duty-cycle used to operate the final array, this value is reduced to 250 ft.L.

3. Electrical Characteristics

Figure 19 shows the current-voltage curve for a typical diode with a dynamic impedance of 10 ohms. To optimize the brightness and hue of the green component, a pulsed voltage of between 6 and 10 volts is normally required. The requirement for a low-resistance ohmic contact of the type discussed in Section IV is demonstrated. For the selected red mode drive condition (1KHz, 1/7 duty cycle) a pulsed voltage of between 2 and 2.5 volts is required.

4. Uniformity Measurements

Figure 20 shows a uniformity map of the 5 x 7 array under optimum red mode drive condition (5mA d.c.). This drive condition ensures that the dominant wavelength of the red/green display most nearly approximates the appearance of a pure red-emitting GaP display (6300Å dominant wavelength); the red mode drive condition of the final Information Display System can sensibly duplicate this performance since the green component has a minor effect on the dominant wavelength at low current densities. Also included in the figure is the uniformity map under optimum green mode drive conditions (2.3KHz, 1/160 duty cycle, 800mA peak current).

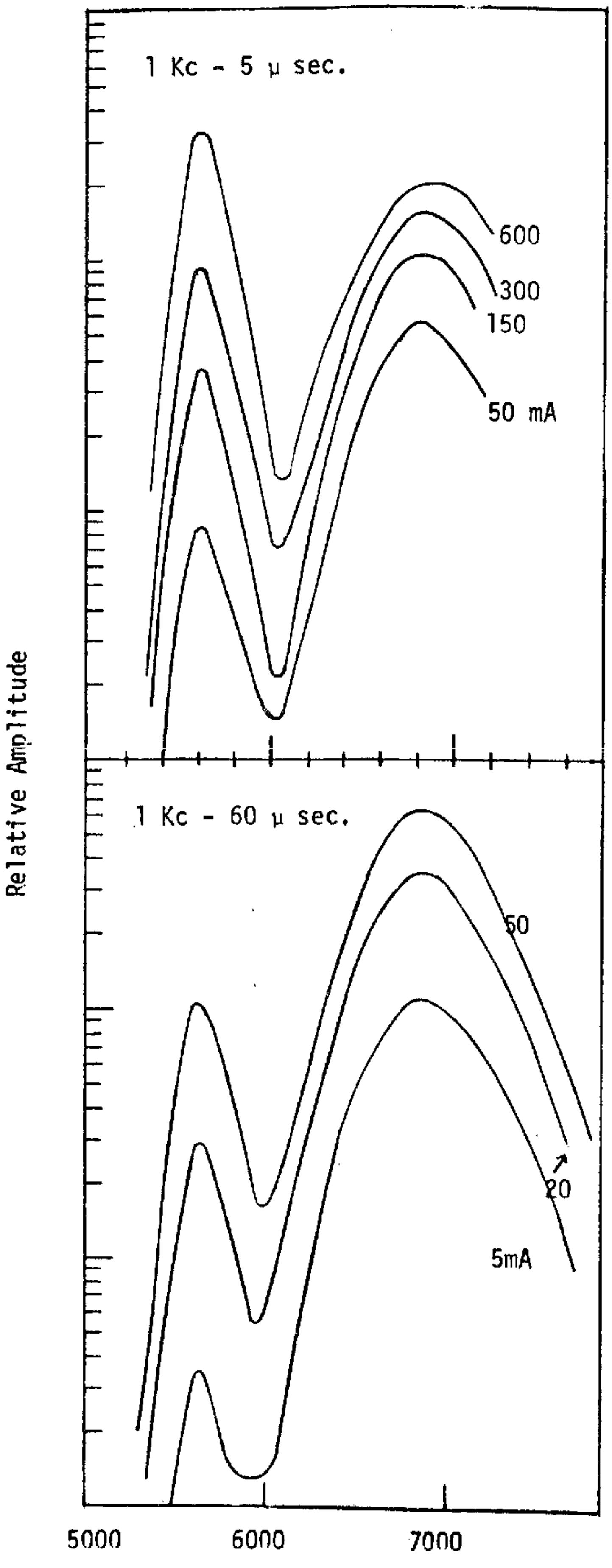

Figure 17 Emission Spectra Of A Typical Multicolor GaP Device. Spectra Are Corrected For Photomultiplier And Grating Response. (Peak Current Is Indicated)

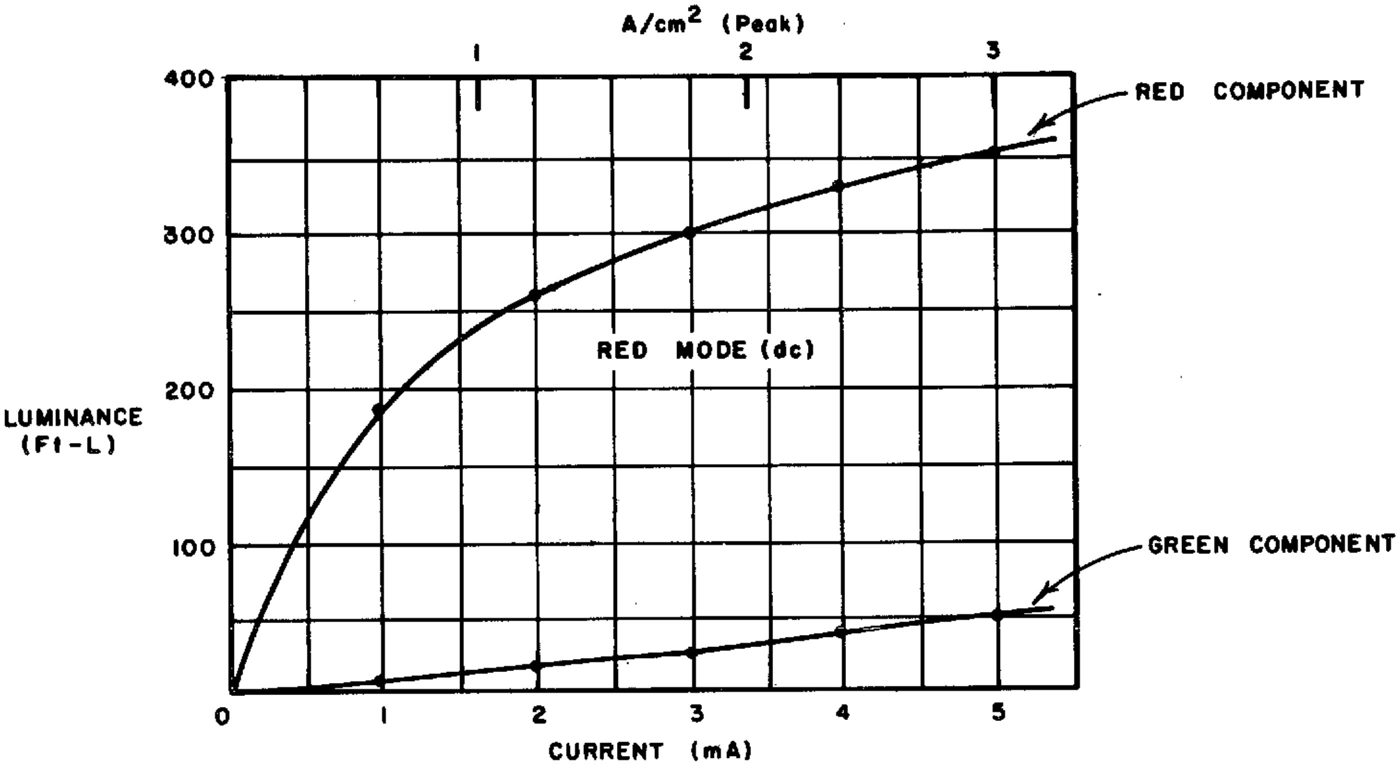

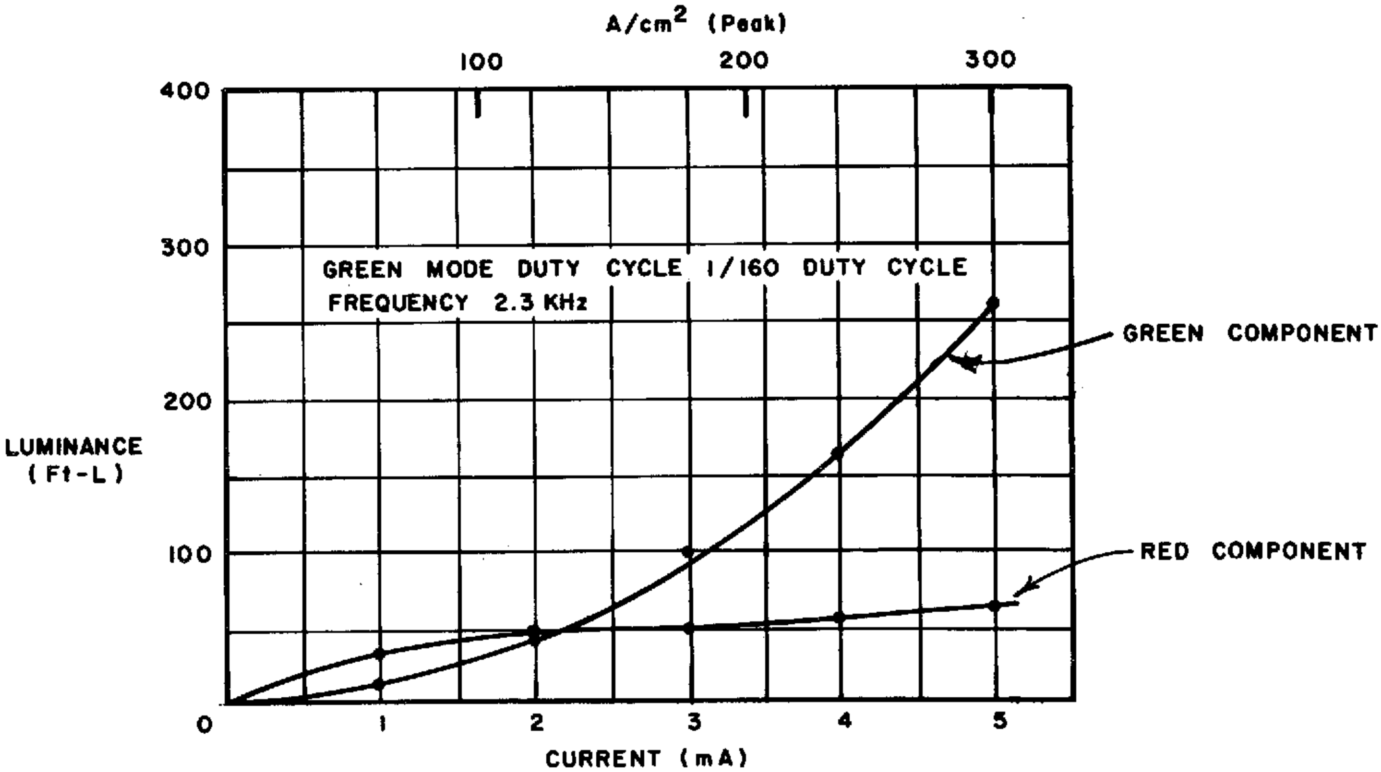

Figure 18 Dependence Of Surface Luminance On Average Operating Current For A GaP Multicolor Display

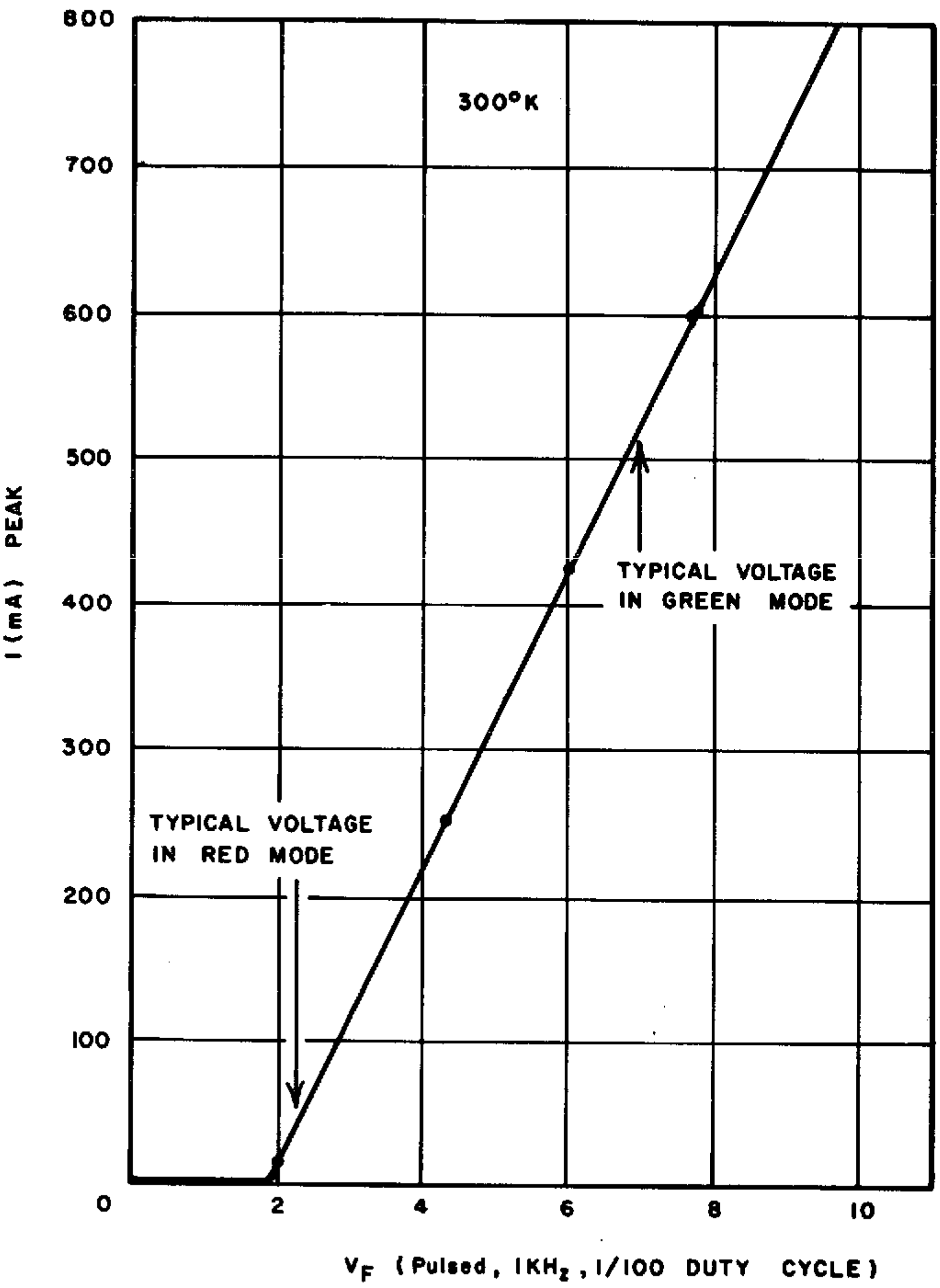

Figure 19 Pulsed V-I Characteristic For A Typical GaP Multicolor Display

405 245	440 265	440 265	415 300	390 250
420 245	420 245	380 300	435 285	405 300
425 265	425 245	400 245	380 250	380 275
430 275	400 245	400 265	380 300	380 285
405 275	430 245	380 265	400 250	380 250
435 265	440 300	400 275	415 300	415 285
430 275	440 275	380 265	420 300	395 290

Figure 20 Emission Uniformity Of A Red/Green Display

(Upper Values Correspond To Total "Red-Mode" Surface Luminance (ft-L) For Elements Operated At 5mA d.c. Lower Values Correspond To Total "Green-Mode"Surface Luminance For Elements Operated At 5mA Average Current (2.3 KHz, 1/160 Duty Cycle)

The emission uniformity, which was measured by integration of diode emission over the entire area of each emitting element, was within the specified $\pm 10\%$ limits for both drive conditions.

The display was not evaluated after its insertion in the completed electronics package, as results are highly dependent on the chosen settings, which, in order to induce a range of dominant wavelengths extending from red through orange and yellow to green, are variable over a wide range of peak current and duty cycle. However, the settings utilized to obtain the above measurements can be approximated in the system delivered to NASA.

5. Contrast Measurements

Contrast measurements were performed on a typical diode under three ambient conditions using a neutral color, circularly polarized filter. For the purpose of these measurements the contrast, C, is taken as

$$C = \frac{E + B}{B}$$

where E is the transmitted brightness of the red/green diode and B is the background intensity incorporating reflections both internal and external to the filter. Results are quoted for the optimum green operating-mode but are applicable across the range of dominant wavelengths. The display fabrication technique discussed previously virtually eliminates optical crosstalk.

(a) 0 foot-candle ambient

- i) Measured element operating only; Contrast $\simeq$ 70:1
- ii) Measured element plus eight nearest neighbours operating Contrast $\simeq$ 35:1

(b) 100 foot-candle ambient

- i) Measured element operating only: Contrast $\simeq$ 12:1
- ii) Measured element plus eight nearest neighbours operating; Contrast $\simeq$ 10:1

(c) 1000 foot-candle ambient

- i) Measured element operating only: Contrast $\simeq$ 2:1
- ii) Measured element plus eight nearest neighbours operating: Contrast $\simeq$ 2:1

Using the circularly polarized filter the reflected background intensity was reduced to 9% of the ambient value.

Contrast measurements were also performed using a louvred filter; this gave generally improved contrast under high ambient levels, but results were highly dependent on the angular distribution of the ambient. Using this filter the reflected intensity was reduced to 2.5% of the ambient in a direction normal to the filter plane.

6. Angular Brightness Variation

Figure 21 shows a polar diagram of intensity versus viewing angle for a typical element of a red/green 5 x 7 array.

7. Lifetest Results

Figure 22 shows a plot of red component and green component intensity (each operating under typical drive conditions) as a function of operating time. As expected, the degradation rate increases at the higher current densities typical of the green operating mode. Improvements in material efficiency and corresponding reductions in the current density required to achieve acceptable green performance are expected to result in extended device lifetimes.

Taking the sensitivity of the eye into account, this degradation would not be expected to cause a noticeable dominant wavelength shift under fixed operating conditions for at least 10,000 hours. This time would be significantly increased under normal operating conditions since any one element would not normally be exercised in the green mode 100% of the time. Independent of current density, no measurable change in the ratio of red:green emission-band intensity was detected over the duration of this lifetest. This infers that the dependence of dominant wavelength on applied current density would remain unchanged over the operating life of the device.

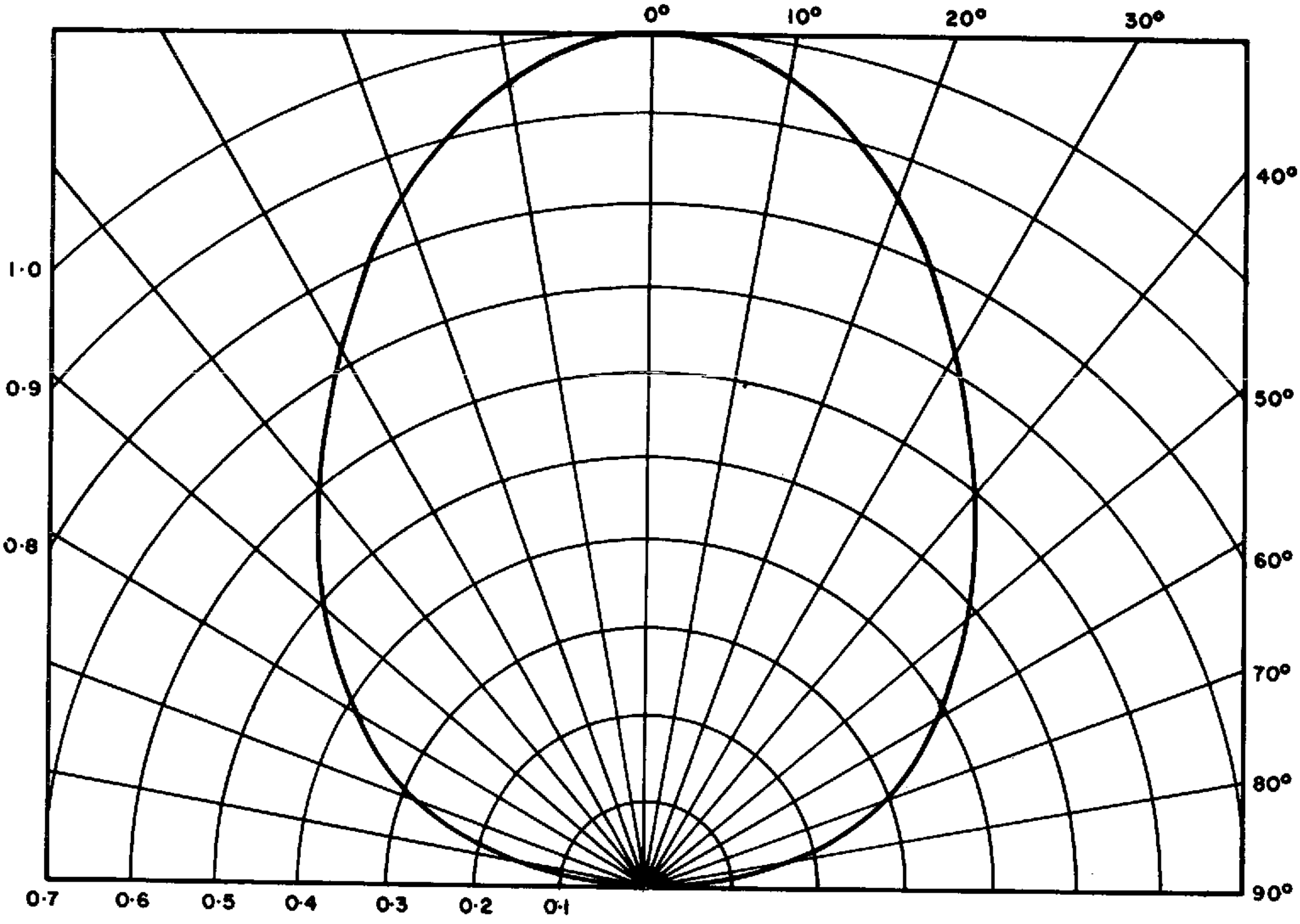

Figure 21 Spatial Brightness Distribution For A Typical Red/Green Element

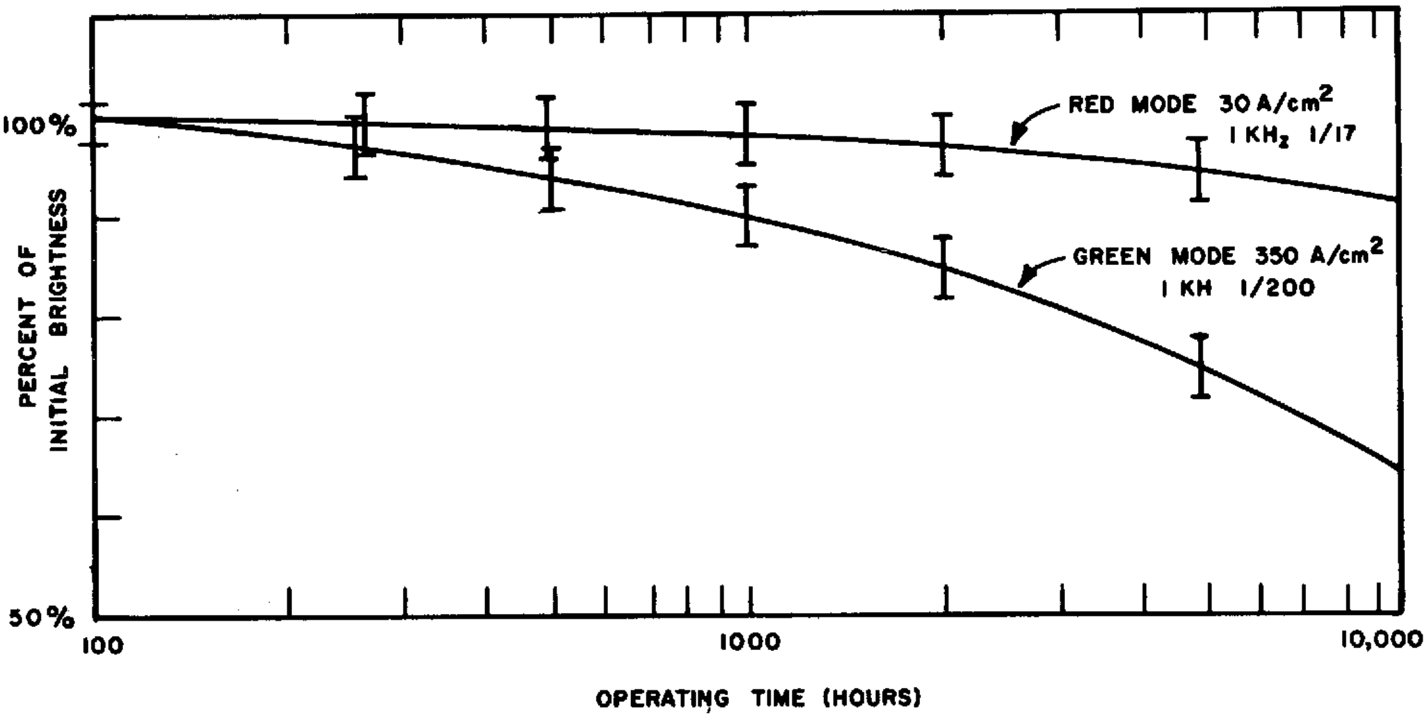

Figure 22 Lifetest Results For A GaP Multicolor Device Under Red-Mode And Green-Mode Drive Conditions

VI DEMONSTRATION ELECTRONICS

In accordance with the program requirements, a demonstration electronics package was designed and constructed for the purpose of demonstrating the alphanumeric and symbolic capabilities of the multicolor 5 x 7 arrays.

Detailed information on the design, operation, and maintenance of the electronics package is included in a manual supplied with the equipment.

The main features of the system and the incorporated displays are reviewed in this section.

The drive circuitry to exercise the 5 x 7 arrays in the complete ASCII code is based on a fixed frequency, variable pulse width, variable current principle. As discussed previously, dominant wavelengths in the red region of the spectrum are generated by operation in a low-duty cycle, low-current mode with the shift towards green dominant wavelengths induced by increasing the peak current applied to the array and simultaneously reducing the pulse width. Display brightness and emission color are controlled by pulse width and pulse height modulation respectively.

The electronics package is designed to receive a 6 bit ASCII word generated either from a computer or its own internal ASCII generator. The state of the word is decoded and then transmitted to the display. The electronics will drive three 5 x 7 red/green arrays plus one green and one red array through a 64-character alphabet.

The five column cathodes are driven on in sequence. The ROM output word is applied to the anode row drivers. Drive is horizontal (column) scan. The duty cycle on the column scan is 1 of 7 with a 1KHz repetition rate.

Pulse width and peak current are adjusted by front panel controls. In the low current or red operating mode, peak current is variable from 5mA to 50mA and the pulse width from 60μ sec. to 200μ sec.; corresponding ranges for the high current or green mode are 100mA - 600mA and 5μ sec. to 20μ sec. The latitude provided in these controls provides for the generation of dominant wavelengths in the red through green region of the spectrum. In addition to the basic red/green format discernible orange and yellow dominant wavelengths can be generated.

A separate front panel control is provided for the following display modes:

Red (orange) only

Green (yellow) only

Green (yellow) on red (orange) background

Red (orange) on green (yellow) background

The alternative dominant wavelengths indicated in brackets are generated by adjustment of the pulse width and peak current controls.

The displays provided with the system include three monolithic multicolor 5 x 7 matrices; details of construction and format were presented in Section IV. To permit evaluation of the influence of emitting element size on display legibility and color characteristics, the emitting element area of one display is masked down from 0.010" to 0.007".

Separate red- and green-emitting GaP matrices are also incorporated in the system; these provide a comparison base for evaluating the color clarity and dominant wavelength range of the multicolor displays. The displays are operated at a fixed pulse width of 100μ sec., and a fixed peak current of 20mA for the red array and 50mA for the green array. The green component of the red array is negligible, resulting in a dominant wavelength of 6300Å. The material selected for the green display was relatively low in nitrogen content; consequently, the shorter wavelength phonon-assisted free exciton recombination dominates the emission spectrum resulting in a dominant wavelength close to 5550Å. The contrast improvement associated with this shorter-wavelength emission color is marked; the red component of the emission spectrum is negligible. Unfortunately for viable multicolor display systems, it is necessary to use material which exhibits the higher-efficiency green-component which is associated with the longer-wavelength, nitrogen-induced recombination.

Each of the three multicolor displays can be individually selected by a front panel control; the single color matrices can be enabled in the red-only mode.

The red and green displays scan in synchronization with the ASCII generator exercising the multicolor matrices; the display rate can be externally controlled, and any word locked in a particular display by means of an external Hold switch.

VII CONCLUSION

The feasibility of utilizing single-junction GaP devices in monolithic, multicolor alphanumeric arrays has been demonstrated.

For this material, dominant wavelengths in the red region of the spectrum were generated by operating under a low current, high duty-cycle mode. Altering the drive conditions to a low duty-cycle, high current mode induced a shift in dominant wavelength towards the green region of the spectrum as a result of the saturation of the red recombination process and the superlinear dependence of the green efficiency on current density. Intermediate drive conditions were used to generate dominant wavelengths perceived as orange or yellow.

Radiative recombination centers associated with efficient red and green emission in GaP were incorporated using liquid-phase-epitaxial (LPE) growth procedures. The most satisfactory performance resulted from a combination of an open-tube dipping technique for n-layer growth and a sealed-tube tipping procedure for p-layer growth. In this method an $n:p^+$ structure was formed in which the n-layer was doped with Te and N and the p-layer with Zn and O_2. The utilization of tipping procedures for n-layer growth resulted in erratic variations in doping levels and surface morphology of nitrogen doped material; this was eliminated by adopting the dipping procedure in which nitrogen doping levels and the distribution of solid phases in the melt was controlled and, in addition, the residual gallium was drained off the surface at termination of growth preventing the regrowth of a highly doped surface layer during quenching. The selected doping levels for the active components were a compromise between the requirements for efficient red and efficient green devices. Extended annealing procedures radically improved the emission efficiency of the red recombination without significantly affecting the green component; these annealing procedures were selectively utilized to optimize the color characteristics of processed material.

Quantum efficiency values for the two components in a typical multicolor display were 1.0 to 1.5% for the red (at a current density of $3A/cm^2$) and 0.01 to 0.02% for the green (at a current density of $250A/cm^2$). Maintaining the same injection characteristics but optimizing the radiative center distribution for either color gave red and green efficiency levels of 2.5% and 0.08% respectively; this efficiency improvement was achieved at the expense of the multicolor capability.

Fabrication techniques for X-Y addressable arrays involved the use of a micro-diamond saw for cathode column isolation and junction delineation. Optical crosstalk was eliminated by screening an opaque epoxy into the isolation grooves and regenerating anode row interconnections by ultrasonic stitch-bonding techniques. The adopting of this technique involved some departure from the concept of a truly monolithic display.

For the fabricated displays surface luminance values in excess of 250 ft-L for both the red and green components were obtained at 5mA average current.

Lifetests showed accelerated degradation rates for devices operated under the elevated peak current drive conditions used to generate a predominant coloration; however, the resulting reduction in lifetime is not considered sufficiently severe to preclude the practical application of this type of device structure.

Anticipated advancements in GaP materials and device technology should result in acceptable multicolor performance at reduced current densities with concomitant improvement in operating lifetime.

For demonstration purposes, an Information Display System incorporating three 5 x 7 multicolor displays and additional "monochromatic" red and green emitting displays was constructed. This system was capable of exercising the displays through the complete 64-character ASCII code in a variety of color combinations and adequately demonstrates the multicolor information display capability of single-junction gallium-phosphide LED arrays.

REFERENCES

1. Morgan, T.N., Welber, B., Bhargava, R.N., 1968, Phys. Rev. 166, 751.
2. Hackett, W.H., Rosenzweig, W.R., and Jayson, J.S., 1969, Proc. IEEE, 57, 2072.
3. Thomas, D.G., Hopfield, J.J. and Frosch, C.J., 1965, Phys. Rev. Lett., 15, 857.
4. Logan, R.A., Rosenzweig, W.R. and Weigman, W., 1971, Solid St. Electron., 14, 655.
5. Weisberg, Leonard R., 1970, Proc. Eighth. Ann. Rel. Phys. Conf. 43, (J.B. Morris, Ed.).
6. Logan, R.A., White, H.G., and Trumbore, F.A., 1965, J. Appl. Phys., 38, 2500.
7. Ladany, I., and Kressel, H., 1972, Final Report CR-112-111, Contract NAS1-10696.
8. Solomon, R., and DeFevere, D., 1972, Appl. Phys. Lett., 21, 257.
9. Saul, R.H., 1972, J. Electron. Mater. 1, 1.
10. Dapkus, P.D., Hackett, W.H. Jr., Lorimor, O.G., Kammlott, G.W., and Hazzko, S.E., 1973, Appl. Phys. Lett., 22, 227.
11. Wight, D.R., Birbeck, J.C.H., Trussler, J.W.A., and Young, M.L., 1973 - to be published.
12. Shih, K.K., Woodall, J.M., Blum, S.E., and Foster, L.M., 1968, J. Appl. Phys., 39, 2962(C).
13. Saul, R.H., 1971, J. Electrochem. Soc., 118, 793.
14. Bacharach, R.Z., and Lorimor, O.G., 1973, Phys. Rev. B, 7, 700.
15. Bacharach, R.Z., Lorimor, O.G., Dawson, L.R., and Wolfstirn, K.B., 1972, J. Appl. Phys., 43, 5098.
16. Dishman, J.M., Daly, D.F., Knox, W.P., 1972, J. Appl. Phys., 43, 4693.
17. Stringfellow, G.B., 1972, J. Electrochem. Soc., 119, 1780.
18. Sudlow, P.D., Mottram, A., and Peaker, A.R., 1972, J. Mater. Sci., 7, 168.
19. Solomon, R., and DeFevere, D., 1972, J. Electron. Mater., 1, 26.

20. Blum, J.M., and Shih, K.K., 1971, Proc. IEEE, 59, 1498.

21. Peters, R.C., 1972, Proc. Fourth Int'l. Conf. on GaAs and Related Compounds, (Inst. of Physics, London).

22. Logan, R.A., White, H.G., and Trumbore, F.A., 1967, Appl. Phys. Lett., 10, 206.

23. Logan, R.A., White, H.G., and Wiegmann, W., 1971, Solid St. Electron., 14, 55.